DOLOMITIZATION AND SULFIDE MINERALIZATION OF LOWER CARBONIFEROUS STRATA, NW IRELAND

By

CHRISTOPHER J. PERSELLIN

Bachelor of Science in Geology

Arizona State University

Tempe, AZ

2006

Submitted to the Faculty of the
Graduate College of the
Oklahoma State University
in partial fulfillment of
the requirements for
the Degree of
MASTER OF SCIENCE
May, 2009

DOLOMITIZATION AND SULFIDE

MINERALIZATION OF LOWER CARBONIFEROUS

STRATA, NW IRELAND

Thesis Approved:

Dr. Jay M. Gregg

Thesis Adviser

Dr. Eliot Atekwana

Dr. Ian Somerville

Dr. James Puckette

Dr. A. Gordon Emslie

Dean of the Graduate College

ACKNOWLEDGMENTS

I would first like to thank the faculty and staff of the Boone Pickens School of Geology at Oklahoma State University for the assistance and opportunities provided during my tenure. I would also like to thank my advisor, Dr. Jay Gregg, for the incredible opportunity this thesis presented, and for all the guidance provided along the way. A special thanks to Dr. Ian Somerville (University College Dublin) for the help during my stay in Dublin, in the field, and for serving as a member on my thesis committee. Thanks to Dr. Eliot Atekwana and Dr. James Puckette for their help with various aspects of the thesis and for serving on my committee. Thanks to Dr. Kevin Shelton (University of Missouri) for the numerous contributions to the project in the field, the lab, and during the writing process. Thanks to John Kelly (JBA Ltd., Dublin) for providing access to the underground workings of Abbeytown Mine and the photographs of the underground workings used in this thesis. I would also like to thank Justin Beasley (University of Missouri) for his help in the field and for giving an introduction to the fluid inclusion measurement techniques and Tom Culligan (University College Dublin) for his help in thin section and fluid inclusion plate preparation. Thanks to the Society of Economic Geologists for providing funding (Hugh E. McKinstry Student Research Award) for this project and Devon Energy for funding my Graduate Fellowship while I attended Oklahoma State. Finally, I want to thank my parents, James and Patricia Persellin, for all of the support they gave me throughout the duration of my graduate studies.

TABLE OF CONTENTS

LIST OF TABLES

Table Page

LIST OF FIGURES

Figure Page

CHAPTER I

INTRODUCTION

The lead-zinc sulfide mineralization at Abbeytown Mine and Twigspark Quarry are the only known carbonate-hosted base-metal sulfide deposits in northwestern Ireland (Fig. 1). Several earlier studies (Oswald, 1955; George *et al*., 1976; Philcox *et al*., 1992; Cózar *et al*., 2005, 2006; Somerville *et al*., in prep.) have focused on defining and correlating the Carboniferous stratigraphy of the region.

Hitzman (1986) investigated the mineralization at Abbeytown and recognized multiple mineralizing events in the deposit by petrographic analyses and fluid inclusion microthermometry. He proposed that the mineralizing fluids were regionally derived basinal fluids that migrated through underlying basal Carboniferous siliciclastic units to the north of Abbeytown (from the Donegal Bay area). Hitzman's (1986) study was limited to the Abbeytown deposit and did not examine other occurrences of base-metal sulfide mineralization in the region (Fig. 2). Alternatively, mineralization in northwestern Ireland also has been attributed to isolated convection cells in which circulating fluids descended extensional faults and interact with basement rocks. After obtaining metal ions from the Proterozoic metamorphic basement, fluids may have used faults and fractures as conduits to ascend to the sites of ore deposition (Russell, 1978; 1986).

Recent studies conducted on Pb-Zn mineralization in the Rathdowney Trend in

the Irish Midlands (Fig. 1) provide evidence for regionally persistent brines derived from seawater evaporated beyond the point of halite precipitation, which mixed on more localized scales with other fluids, some of which likely circulated through basement rocks (Banks *et al*., 2002; Nagy *et al*., 2004; Wilkinson *et al*., 2005; Johnson *et al*., in press). Several studies have shown that as many as three chemically distinct fluids were involved in regional mineralization (Gregg *et al*., 2001; Johnson *et al*., in press). The tectonic isolation of the mineralization in northwest Ireland from the mineralized regions in the Irish Midlands provides an ideal opportunity to investigate the fluid system and sulfide mineralizing events in a relatively isolated area (Fig. 1).

The purpose of this study is to examine regionally distributed epigenetic cements within the Sligo Syncline of northwestern Ireland to: (1) identify the source of mineralizing fluids at each locality and determine whether they are regionally distributed basinal brines, locally convected hyrothermal fluids, or some combination of these; (2) characterize the fluid history and diagenetic sequences observed at each locality; and (3) determine if, and to what extent, hydrologic connectivity between localities occurred during mineralization. Developing the fluid migration history in northwest Ireland will aid in understanding the genesis of Abbeytown Mine and may have applications to other carbonate-hosted base-metal sulfide deposits in similar geologic settings.

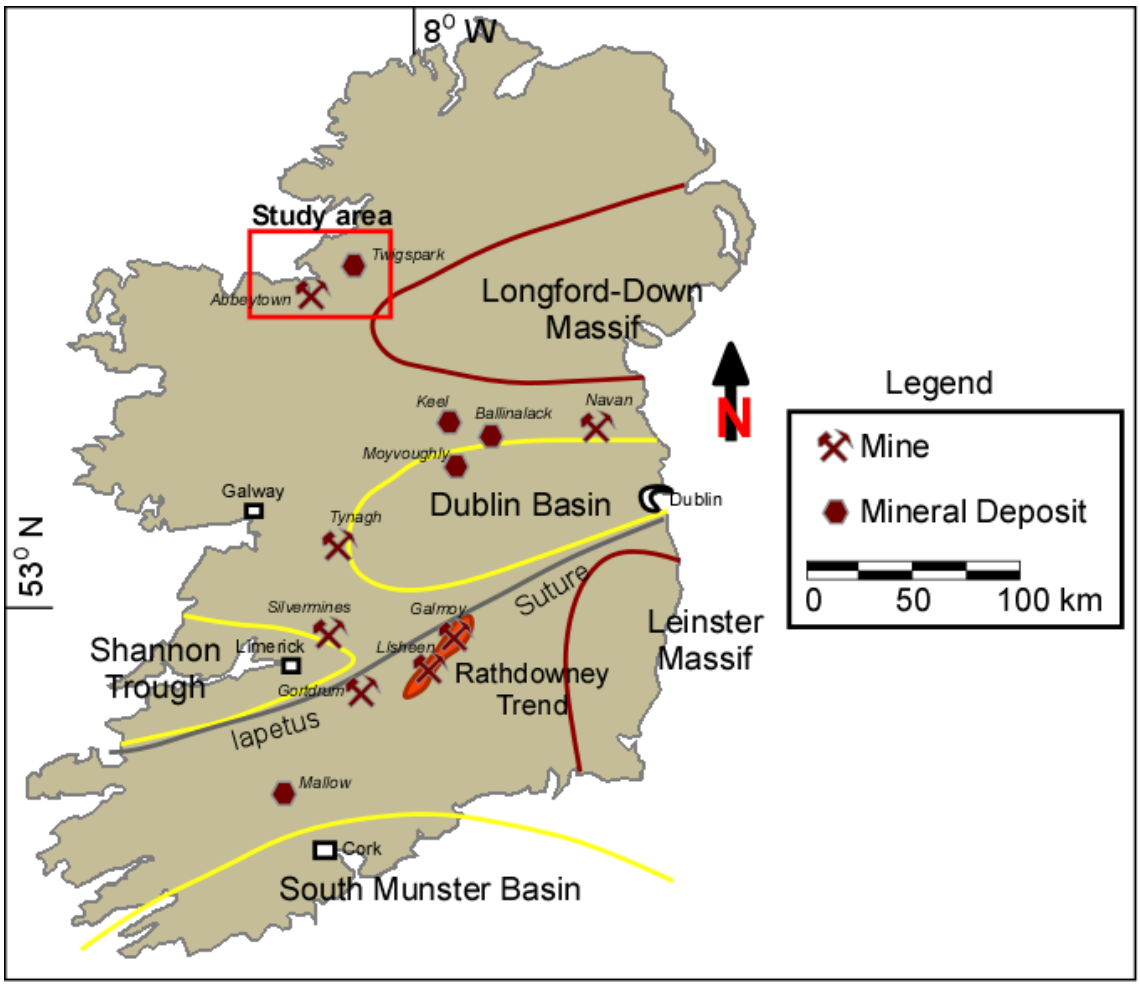

Figure 1. Map of the major tectonic provinces and sedimentary basins of Ireland. The region of study is indicated. Modified from Gregg *et al*. (2001).

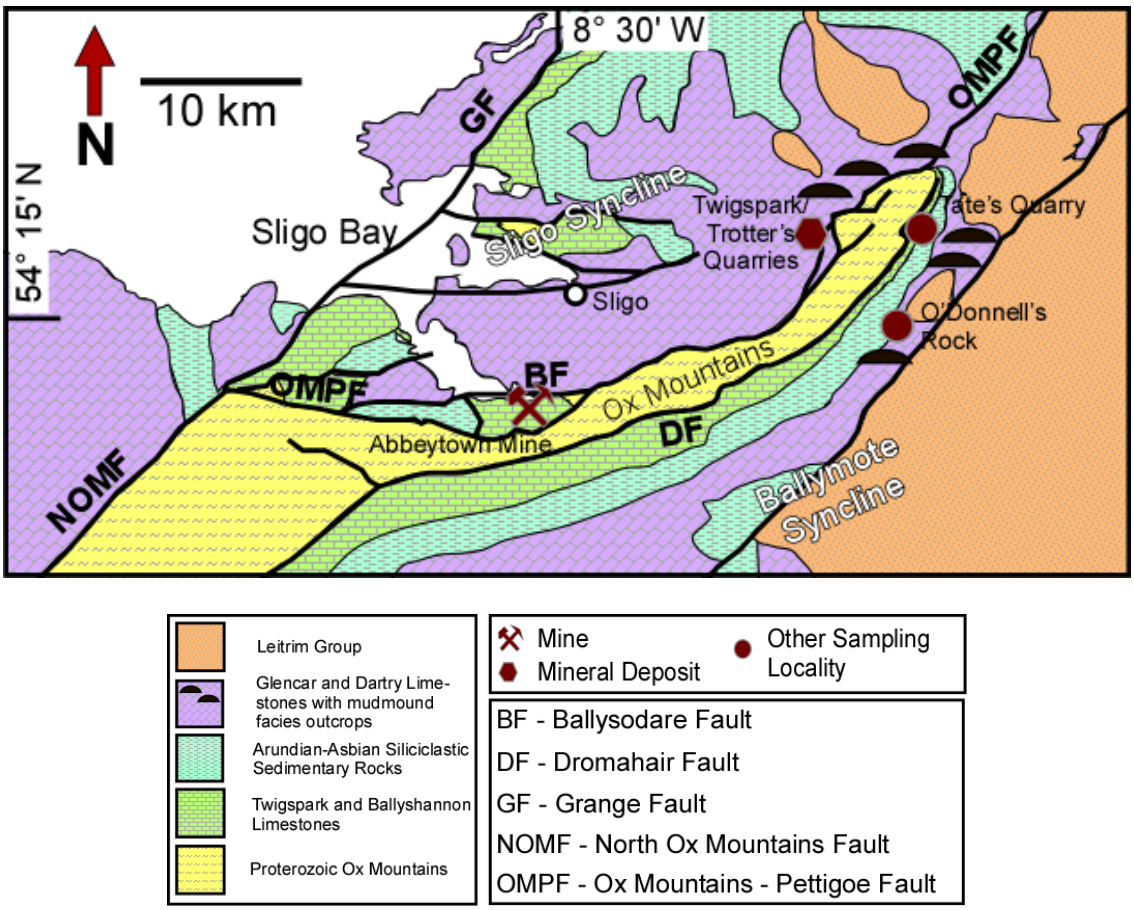

Figure 2. Geologic map of northwestern Ireland. Sample localities are indicated. Modified from MacDermot *et al*. (1996); 1:500,000 GSI Bedrock map of Ireland.

CHAPTER II

GEOLOGIC SETTING

Structure

The region of base-metal sulfide mineralization in northwest Ireland is isolated structurally from carbonate-hosted mineralization in the Irish Midlands, and is related geographically to the Ox Mountains uplift (Fig. 2). The Ox Mountains are bounded by two regional normal faults; on the southeast by the Dromahair Fault (DF) and on the northwest by the Ox Mountains-Pettigoe Fault (OMPF). A series of E-NE striking, high-angle faults transect the Sligo Syncline to the west of the Ox Mountains, extending into Sligo Bay. Between these high-angle faults, Carboniferous strata are folded broadly, displaying a wide range of dip angles and directions. Movement along faults within the Sligo Syncline is believed to have commenced during the Lower Carboniferous with significant thickness variations observed in the Benbulben Shale, Glencar Limestone, and Dartry Limestone formations possibly as a result of syn-sedimentary faulting (Hitzman, 1986; Somerville *et al*., in prep.). Evidence for reactivation of basement faults during the Late Carboniferous has been identified in some areas of the northwest Ireland region (Price and Max, 1988; Mitchell, 1992).

The Pb-Zn deposit at Abbeytown is bounded between two significant faults, the OMPF to the south and the east-trending Ballysodare Fault to the north (Fig. 2). Hitzman

(1986) observed that the smaller western ore body was more closely related to the presence of a high-angle reverse fault, the Abbeytown Fault, and the eastern ore body was related to an asymmetric syncline within the fault-bounded block (Figs. 3 & 4). The ore bodies are separated by approximately 150 m. Twigspark Quarry is located along the northern extension of the OMPF, 20 km northeast of Abbeytown (Fig. 2).

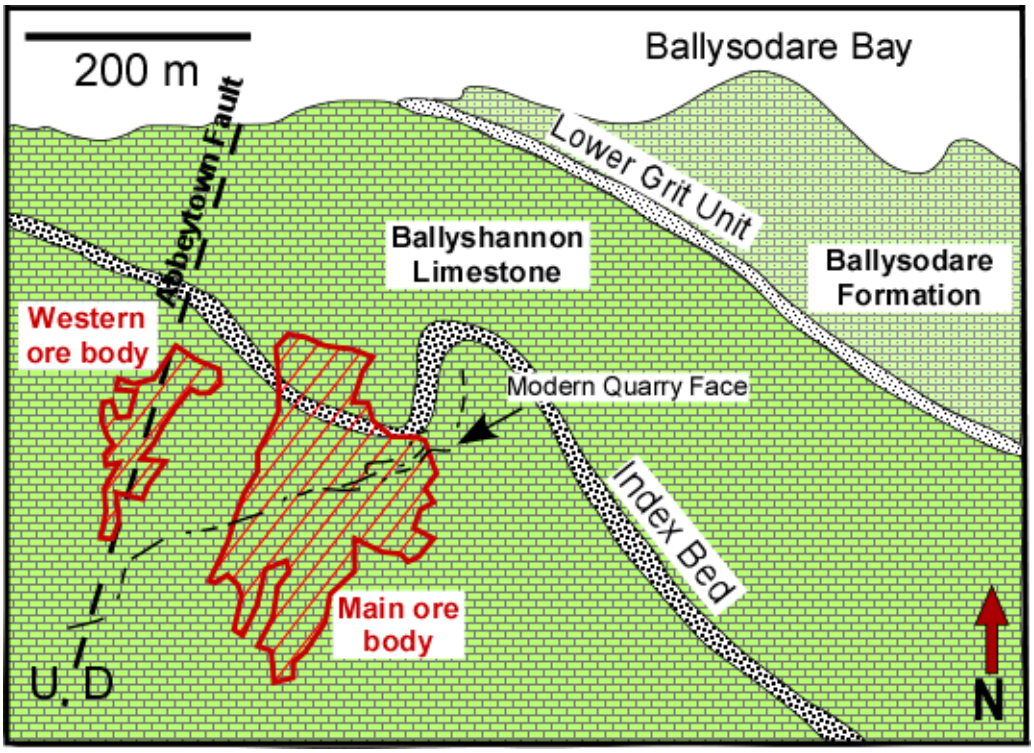

Figure 3. Local map of Abbeytown Mine area. The extent of old mine workings and modern quarry face are indicated. Modified from Hitzman (1986) and Kelly (2007).

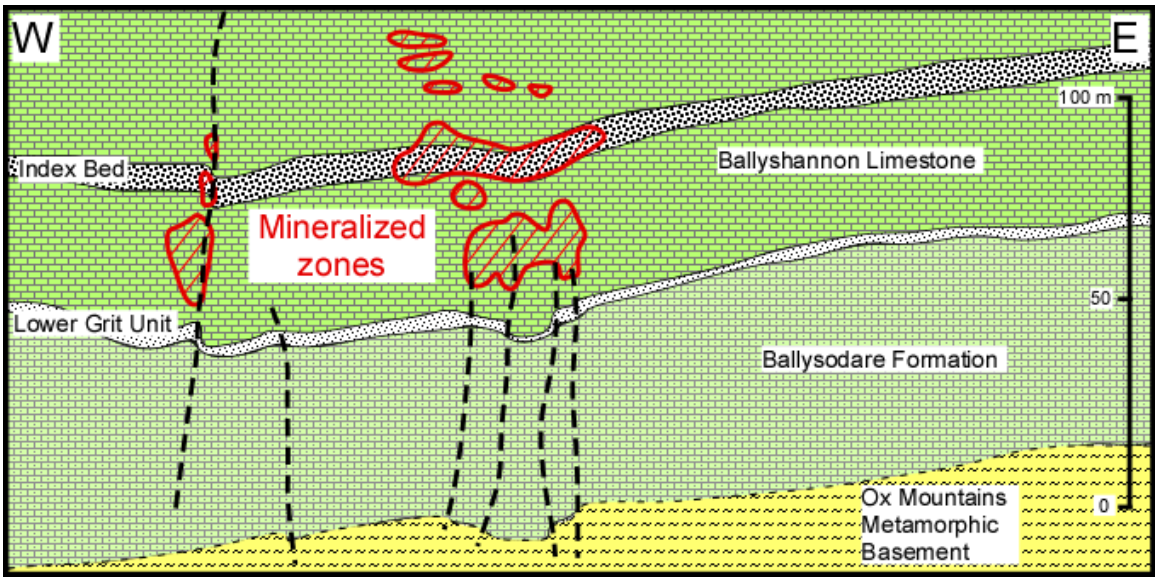

Figure 4. Generalized cross section of Abbeytown Mine area. Location, orientation, and depth of penetration of faults are inferred from cores drilled in the mine area. Modified from Hitzman (1986).

Basement Geology

Comprehensive petrographic examinations of the basement rocks of northwestern Ireland is found in Molloy and Sanders (1983), Johnston (1995a), MacDermot *et al*. (1996), and Thomas *et al*. (2004). The Proterozoic and Lower Paleozoic geology of Ireland was shaped by the deposition and subsequent deformation of an assortment of different terrains (Johnston, 1995b). The rocks of the Ox Mountains Inlier display varying degrees of metamorphism ranging from greenschist to amphibolite, and rarely blueschist facies (Rayner, 1981; Chew *et al*., 2003). Rocks of the older Slishwood Division consist of paragneisses, micaeous quartzites, and feldspathic psammites. The younger Dalradian Supergroup contains a variety of schists, including mica, chlorite, and garnet schists, along with layers of quartzite and marble (Charlesworth, 1953; Johnston and Phillips, 1995). Deformation is correlated to the Grampian and Taconic orogenies, with additional alteration to the southwest produced by the Caledonian orogeny (Johnston, 1995b).

Carboniferous Stratigraphy

Detailed examinations of the Carboniferous stratigraphy in northwestern Ireland is found in Oswald (1955), George *et al*. (1976), Hitzman (1986), Philcox *et al*. (1992), MacDermot *et al*. (1996), Cózar *et al*. (2005, 2006) and Somerville *et al*. (in prep.). The northwest was the last region of Ireland to be submerged by a northward-transgressing sea during the late Devonian and early Carboniferous. The basal Twigspark Formation was defined by Philcox *et al*. (1992) from cores and quarries, as a basal sandstone (Fig.

5) and sandy limestone (10-20 m thick) overlain by approximately 35 m of argillaceous micrites and capped by oolitic sandstones. An age-equivalent unit of similar lithology is informally termed the Ballysodare Limestone (Fig. 5) with limited surface exposures near the Abbeytown Mine (Hitzman, 1986).

Overlying the Twigspark Formation is the Chadian-Arundian Ballyshannon Limestone that hosts Pb-Zn mineralization in the Abbeytown area. The Ballyshannon Limestone is marked at its base by the Lower Grit Unit, composed of a 1-2 m thick pebbly calcarenite and overlain by 60 m of fine calcarenites with interbedded shales (Fig. 3). The lower calcarenites and shales are overlain by dark, fine-grained crinoidal packstones with chert nodules and interbedded shales totaling a gross thickness of approximately 200 m (Philcox *et al*., 1992; MacDermot *et al*., 1996). Approximately 40 m above the base of the Ballyshannon Limestone is the 5-7 m thick Index Bed (Fig. 5), a calcareous sandstone to fine-grained conglomerate cemented by carbonate and sulfide minerals (Fig. 6). The Index Bed serves as a marker bed in the Abbeytown area due to the high abundance of detrital quartz and feldspar grains along with significant mica grains present. The lateral extent of the Index Bed is uncertain.

By the late Arundian, the lithology transitioned to mud-dominated sediments due to a period of uplift to the north. The siliciclastic stratigraphy overlying the Ballyshannon Limestone consists of the poorly exposed and highly fossiliferous Bundoran Shale (calcareous mudstone), the Mullaghmore Sandstone (medium-grained sandstone to silty mudstone), and the Benbulben Shale (calcareous mudstone). A gradual transition occurs from the Benbulben Shale to shelf carbonate deposits with some interfingering present (Philcox *et al*., 1992).

Carbonate deposition resumed with the Asbian Glencar Limestone (cyclic argillaceous limestone) and Dartry Limestone (carbonate mudmounds and cherty limestones). During deposition of these units, the region was a continuous carbonate shelf (Somerville *et al*., in prep.). Following a period of uplift and erosion, the Meenymore Formation was deposited over the Dartry Limestone to the east and southeast of the Sligo Syncline (east of the Ox Mountains Inlier) marking the base of the Leitrim Group siliciclastic succession (Somerville *et al*., in prep.). The Meenymore Fm consists of thin-bedded carbonate deposits, laminated shales, fluvial sandstones and two distinct evaporite deposits (West *et al*., 1968; Philcox *et al*., 1992). The presence of evaporite minerals and preserved mudcracks indicate periodic exposure in an intertidal depositional setting.

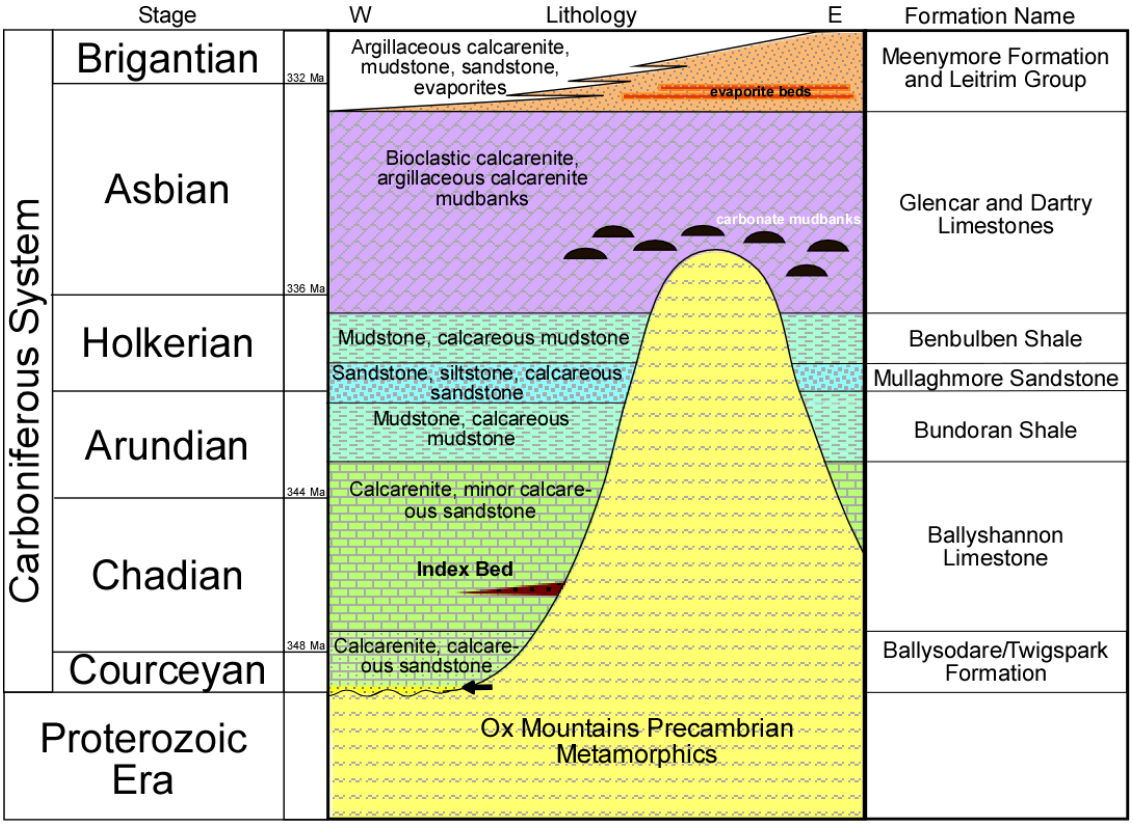

Figure 5. Simplified stratigraphic section of northwest Ireland. Arrow indicates thin (3-4 m) siliciclastic unit at base of Twigspark Formation. Stage ages are from Menning *et al.* (2006).

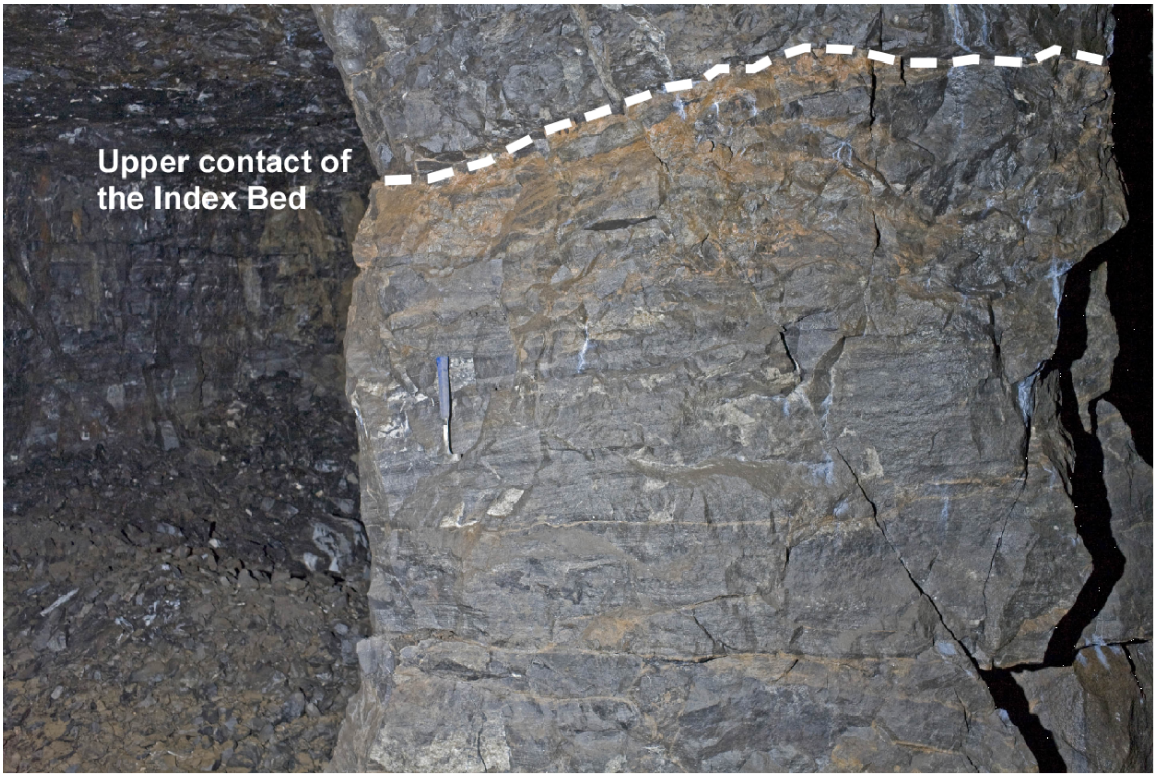

Figure 6. Contact at the top of the Index Bed with overlying Ballyshannon Limestone in a pillar in the main orebody at Abbeytown. Cross bedding is evident near the hammer. Brown coloration is sphalerite mineralization. The rock hammer for scale is approximately 30 cm. (Photo by John Kelly)

Mineralization

Documented mining activity at Abbeytown occurred intermittently from the 1700s until 1961 with about 1.1 Mt of 5.3% lead and zinc recovered (Hitzman, 1986; Kelly, 2007). Kelly (2007) provides a detailed account of mining activity, production, and development. Hitzman (1986) and MacDermot *et al*. (1996) present descriptions of the geology of the Abbeytown deposit. Sulfide mineralization at Abbeytown Mine consists of galena, sphalerite, and pyrite. Distribution of these minerals is dependent on stratigraphic location relative to the Index Bed. Below the Index Bed mineralization is primarily galena, within the Index Bed mineralization is dominantly sphalerite, and above the Index Bed pyrite is more abundant. Sulfide mineralization is linked generally to the distribution of dolomitized host rock in the main ore body; however some late-stage pyrite is present in calcite breccias. Sulfide mineralization and dolomitization is related locally to structural features such as the Abbeytown Fault (Fig. 3) and is most widespread laterally within and adjacent to the Index Bed, where detrital quartz and feldspar grains created enhanced porosity and permeability relative to the surrounding limestone strata.

Minor sulfide mineralization at Twigspark Quarry consists of sphalerite, galena, pyrite, and chalcopyrite. Mineralization at Twigspark has generally been overlooked by previous studies, though MacDermot *et al*. (1996) suggests that mineralization occurs in northeast-trending veins parallel to small faults in the area. Trace pyrite and sphalerite were observed in this study at multiple stratigraphic intervals in cores from near the Twigspark Quarry. The lateral extent of the mineralized zone is uncertain, although additional exploration in the area has been unsuccessful.

CHAPTER III

SAMPLING AND METHODS

Sample Localities

Thin sections were prepared from 74 samples collected from four localities in northwestern Ireland (Fig. 2, Appendix 1). The sample localities were selected to include known sulfide mineralization in the region and to allow for the development and examination of geographic and stratigraphic relationships. An emphasis was placed on collecting samples showing dolomitization, void-filling carbonate cements, and sulfide mineralization.

A total of 26 samples were collected from Abbeytown Mine and Quarry, 18 from the main ore body and 8 from the smaller, western ore body (Fig. 3). An additional 8 samples were obtained from the nearby ABC-8 core originally sampled by Wright (2001) (Appendix 2). Samples obtained from Abbeytown Mine provide coverage of both the main and western ore bodies from both the surface quarry and underground mine (Fig. 7 A-B).

Seven samples were selected from the Abbeytown Mine and Quarry for fluid inclusion analysis (Appendix 3). Dolomite cement is present in 4 analyzed samples, sphalerite was analyzed in 3 samples, and calcite cement is present in 5 samples. Two dolomite samples from both the main and western ore bodies were analyzed. Four calcite

samples are from the main ore body with coverage below, within, and above the Index Bed. One sample is from the western ore body. A total of 82 dolomite-hosted inclusions, 89 calcite-hosted inclusions, and 30 sphalerite-hosted inclusions were measured.

Seventeen samples were selected from two surface quarries to the northeast of Abbeytown; Trotter's Quarry and the nearby Twigspark Quarry (TWC/TQ) (Fig. 7 C-D). An additional 11 samples were obtained from three cores extending to the Proterozoic basement drilled near Twigspark Quarry (Fig. 2). The cores extend down through Ballyshannon Limestone equivalents before encountering basement schists at depths of 310-410 m (Appendix 2).

Five samples from the TWC/TQ area were analyzed for fluid inclusions; epigenetic dolomite cement was present in three samples, and blocky calcite cement was present in four samples (Appendix 3). The samples containing dolomite cement covered a range of stratigraphic levels; one was obtained from Trotter's Quarry at the surface, another from a depth of 155 m, and the third from a depth of 319 m in borehole #TP96-3. Four samples containing calcite cements were observed, two from surface localities and two from Twigspark core #TP96-3. The core samples contain both dolomite and calcite cements; the surface samples contain only calcite cements. A total of 73 inclusions in dolomite and 51 inclusions in calcite were measured.

Five samples were obtained from O'Donnell's Rock, which contain dolomite, calcite, and authigenic quartz cements (Figs. 2 & 7F). Samples from O'Donnell's Rock encompass the uppermost Glencar Limestone and extend into the basal Dartry Limestone. Three samples were selected from O'Donnell's Rock for fluid inclusion analysis (Appendix 3). One sample contains a vug lined with dolomite rhombs and filled in the

center with calcite. Another sample contains a calcite-filled vug. The final sample contains a large vug filled by authigenic quartz. A total of 26 inclusions in quartz, 8 inclusions in dolomite, and 14 inclusions in calcite were analyzed.

At Tate's Quarry, age equivalent beds of the Ballyshannon Limestone to the east of the Ox Mountains Inlier were sampled. Six samples were collected from Tate's Quarry which contain calcite and fluorite mineralization (Figs. 2 & 7E). Two samples were selected from Tate's Quarry for fluid inclusion analysis (Appendix 3). One sample contains both calcite and fluorite cements, the other sample contains only calcite. A total of 32 inclusions in calcite and 33 inclusions in fluorite were measured.

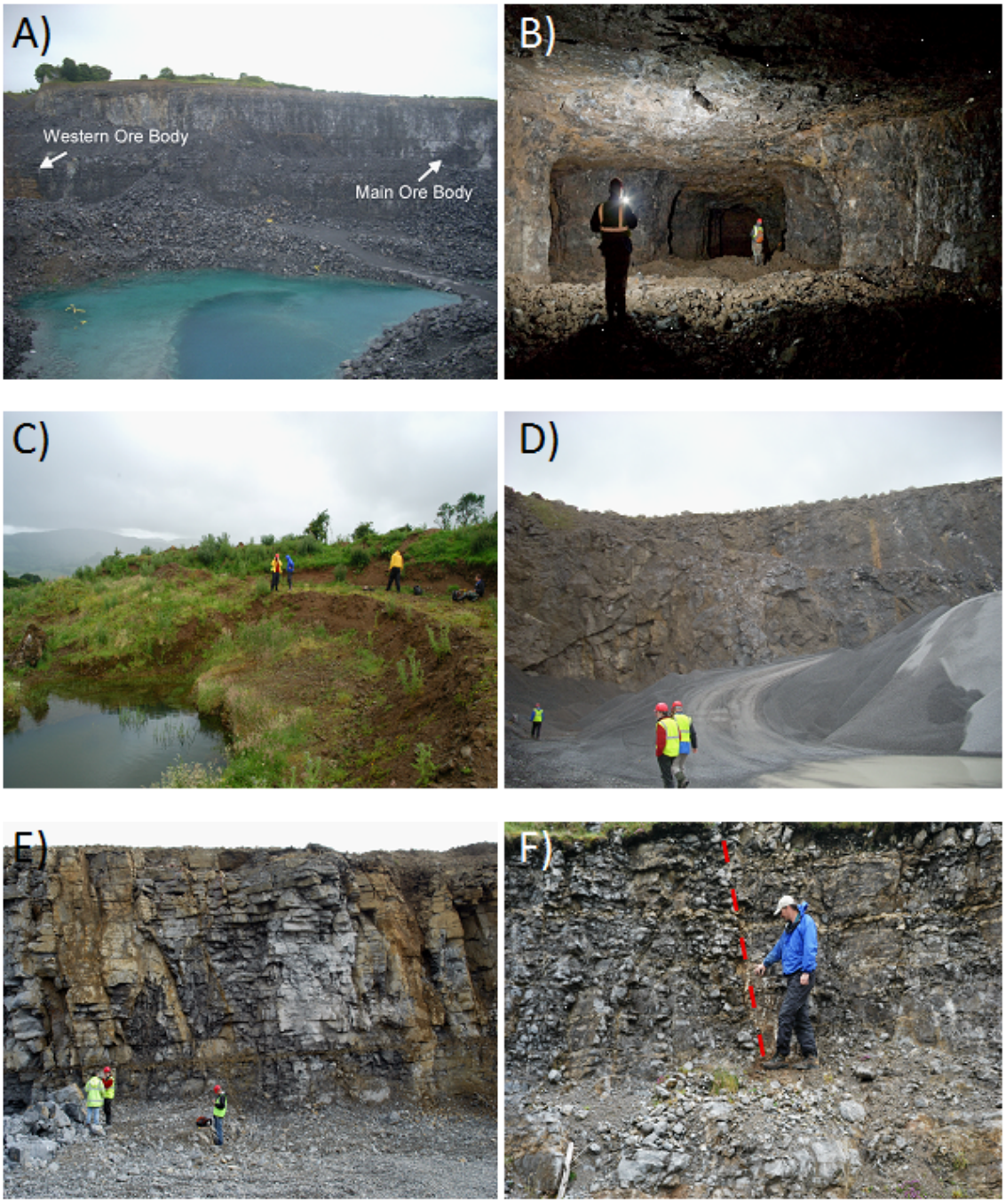

Figure 7. A) Abbeytown Mine Quarry (view facing north) in the Ballyshannon Limestone, with relative locations of the main and western ore bodies indicated. B) Photograph of the underground portion of Abbeytown Mine (photo by John Kelly). Pillar height is approximately 3.5 m. C) Twigspark Quarry. D) Massive mud mound facies of Dartry Limestone at Trotter's Quarry. E) Well-bedded Ballyshannon Limestone at Tate's Quarry. F) Normal fault (red) with approximately 15 cm of offset in bedded Dartry Limestone at O'Donnell's Rock. The normal fault is striking 355° and dipping 71°W.

Laboratory Methods

Cathodoluminescence petrography of dolomite and calcite cements was conducted using a CITL CL8200 MK5-1 Optical Cathodoluminescence System. Photomicrographs were obtained with a Q Imaging Micropublisher 5.0 RTV cooled camera mounted on an Olympus BX51 petrographic microscope.

Fluid inclusion microthermometric measurements were carried out using a Linkam THMSG 600 heating and cooling stage with an Olympus Q Color 3 camera. Temperatures of homogenization (T_h) and ice melt (T_m) have errors of ±1.0 °C and ±0.3 °C respectively, based on reproducibility of data. The inclusions measured were two-phase, primary and pseudo-secondary inclusions, as defined by Goldstein and Reynolds (1994). Salinities were calculated from T_m measurements using equations from Bodnar (1992). No daughter minerals were present in any inclusions, and no vapor-rich (>10%) inclusions were observed.

Carbon and oxygen isotope compositions of carbonates were determined using a Thermo-Finnigan Delta Plus gas-source mass spectrometer with a Kiel device at the University of Missouri (Appendix 4). The $\delta^{13}C$ and $\delta^{18}O$ values (VPDB) have standard errors of less than ±0.05‰ and have been corrected for reaction with 103% phosphoric acid at 70°C (Rosenbaum and Sheppard, 1986). An emphasis was placed on selecting samples for isotope analysis for which fluid inclusion data were available.

CHAPTER IV

RESULTS

Abbeytown

Petrography

The host Ballyshannon Limestone at the Abbeytown Mine is fossiliferous and contains pelloidal packstones and grainstones. Replacement dolomitization in the Abbeytown Mine and Quarry area is generally limited to the main ore body and is contained within and adjacent to the Index Bed. The western ore body is undolomitized to partially dolomitized near the Abbeytown Fault, except for the presence of epigenetic open space-filling dolomite cements. Replacement dolomite is commonly dark gray, coarsely crystalline (2-4 mm), and nonplanar, although some planar-s type dolomite is present (Fig. 8 A-B) (classification of Sibley and Gregg, 1987). The primary pelloidal texture of the limestone has been preserved through dolomitization.

Carbonate cementation in the Abbeytown area occurs in fractures, joints, and vugs. Calcite cement in fractures and vugs is composed typically of large, blocky crystals (Fig. 8 C-D). Dolomite cements filled early porosity and occur as two forms: 1) large, white to pink to brown, saddle dolomite crystals and 2) fine-grained, grey, planar-e, vug-filling dolomite cement (Fig. 9 A-B).

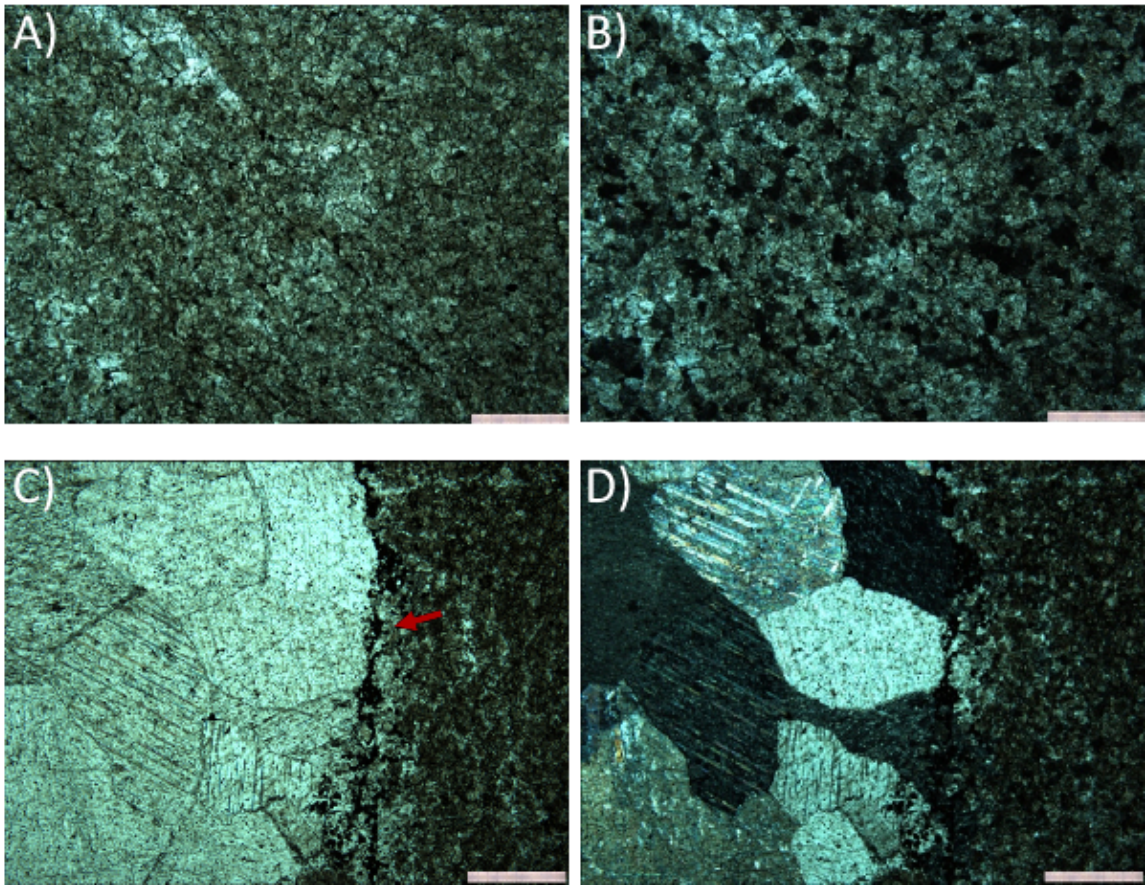

Figure 8. A) and B) Dolomitized host rock from Abbeytown Mine in plane-polarized light (PPL) and cross-polarized light (XPL), respectively [AT-8]. Scale = 1 cm. C) and D) Large (> 1 cm) calcite cement in a vein in PPL and XPL views [AM-4]. Dolomitized host rock is shown on the right. Note the thin zone of galena lining the vein (depicted). Scale = 1 cm.

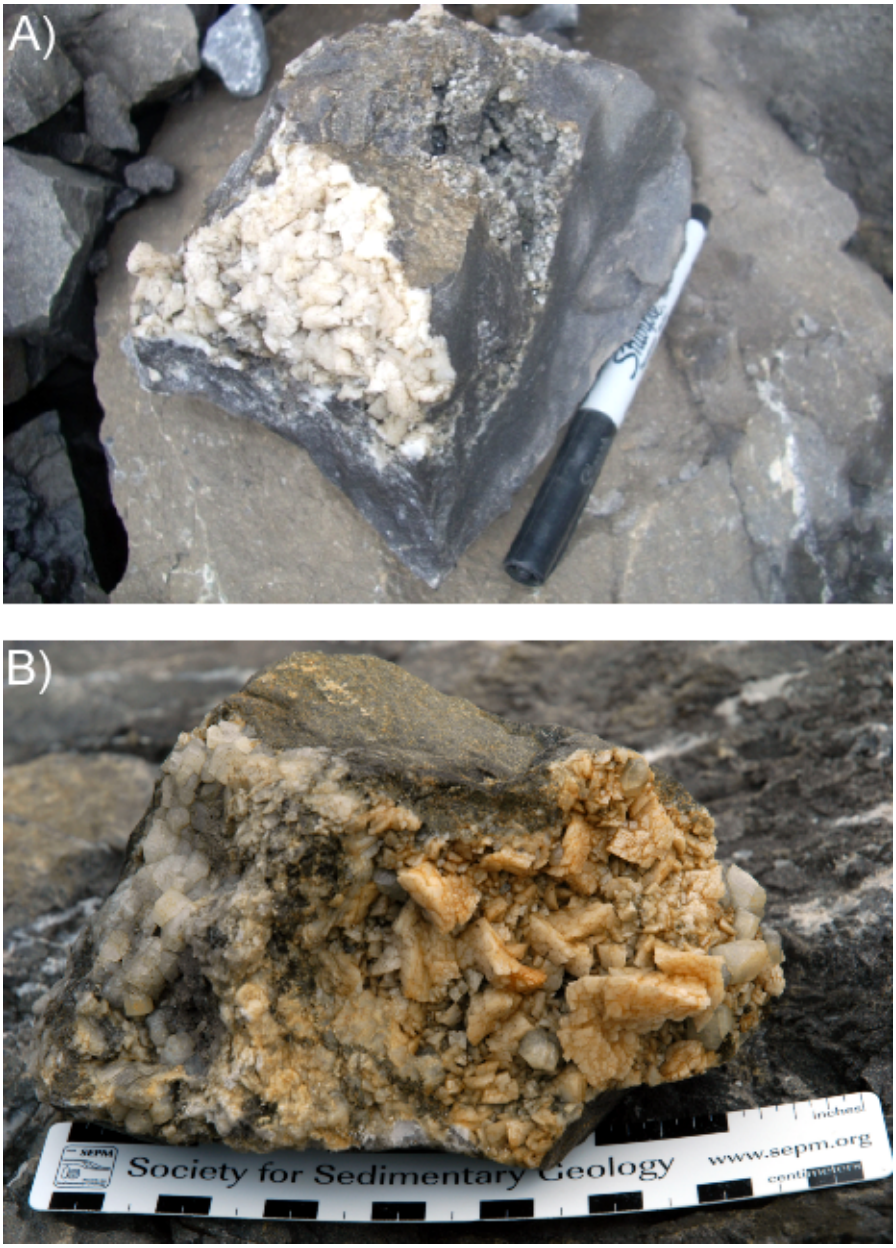

Figure 9. A) Hand sample showing two types of dolomite cements at Abbeytown: large (cm-scale), white-pink saddle dolomite (left) and small (< 1 cm), grey dolomite rhombs (right) [AM-11]. B) Large, white-brown saddle dolomite (right) with white calcite cements (left) from Abbeytown Mine [AM-10].

Cathodoluminescence

At Abbeytown a four zone cathodoluminescence (CL) microstratigraphy was identified in replacement dolomites: Z1: a black, non-luminescent core, Z2: a thin, brightly luminescent band, Z3: a wide, poorly luminescent to non-luminescent zone, and Z4: a thin, bright outer rim (Fig. 10 A-B). Dolomite collected below the Index Bed commonly has much thinner Z3, and Z4 is absent in these samples (Fig. 10 C-D). In three samples, a moderately luminescent mottled core is present, followed by Z1-Z4.

There is a common CL microstratigraphy present in dolomite cements at Abbeytown consisting of three zones (Fig. 10 E-F) followed less commonly by a fourth outer zone. CZ1 is a moderately luminescent, mottled core, CZ2 is a wide, moderately to non-luminescent zone, CZ3 is a brightly luminescent, typically thin band, and CZ4, where present, is a multi-banded, luminescent zone. Three samples contain dolomite cements with CL microstratigraphies differing from that described here. Two of these samples display a non-luminescent core, a wide, darkly luminescent middle zone and a non-luminescent outer zone. The third sample contains dolomite cement that was uniformly non-luminescent. There is no apparent geographic or stratigraphic relationship among these anomalous samples.

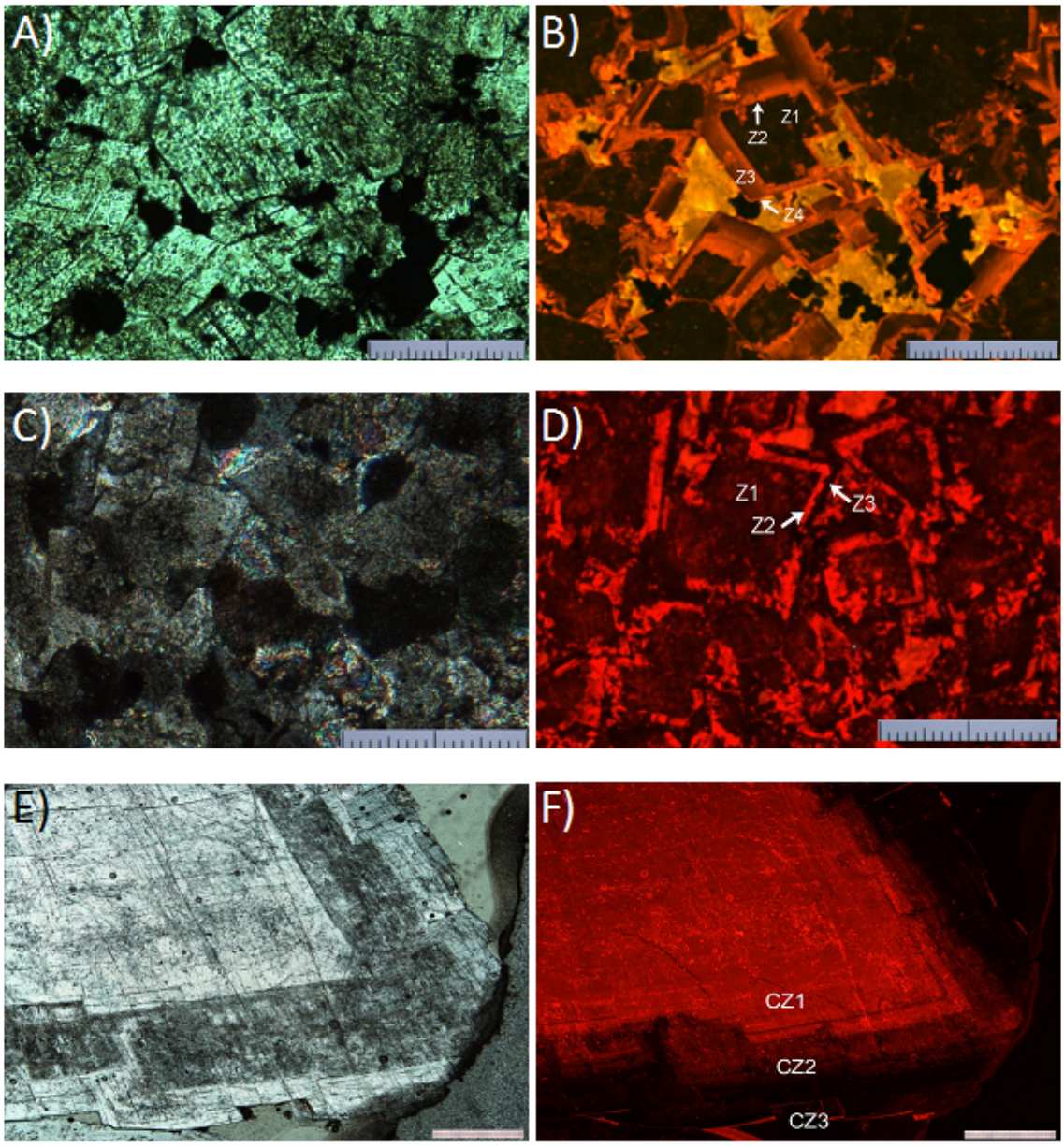

Figure 10. A) and B) PPL and CL photomicrographs of zonation in replacement dolomite from Abbeytown, above the Index Bed [AM-13]. Z1-Z4 shown. Orange luminescence is calcite formed from dedolomitization. Opaque mineral in PPL photo is pyrite. Scale = 2 mm. C) and D) XPL and CL photomicrographs of replacement dolomite below the Index Bed [AM-8]. Note the absence of Z4 and abbreviated Z3. Scale = 2 mm. E) and F) PPL and CL photomicrographs of zoned saddle dolomite cement, showing CZ1-3 [AM-11]. Scale = 1 cm.

Paragenesis

Sedimentation in the Abbeytown area was dominated by carbonate for much of the Lower Carboniferous, with a period of increased siliciclastic input resulting in the formation of the Index Bed (Fig 5). Initial cementation of fractures by calcite likely occurred prior to dolomitization (Fig. 11A). Laterally extensive dolomitization is present only in proximity to the Index Bed (Hitzman, 1986). A zone of partial dolomitization forms a halo further from the synclinal structure in the Abbeytown Mine area. An early sulfide mineralizing event, possibly correlative with the initial dolomitization, resulted in the formation of early sphalerite and pyrite (Fig. 11A). The early mineralization was limited to the Index Bed and underlying carbonates immediately adjacent to the Abbeytown Fault.

Formation of large saddle dolomite cements followed the initial sulfide mineralization event and preceded the episode of main sulfide mineralization. The main sulfide mineralization event (Fig. 11A) resulted in the formation of Pb-Zn sulfides adjacent to the Abbeytown Fault in and below the Index Bed. Minor partial dedolomitization is likely tied to the precipitation of late, blocky calcite cements. Pyrite is typically found associated with calcite cements in breccias, and is limited stratigraphically to above the Index Bed. Dissolution of detrital grains, mostly feldspars, and late fracturing resulted in post mineralization secondary porosity in the Index Bed.

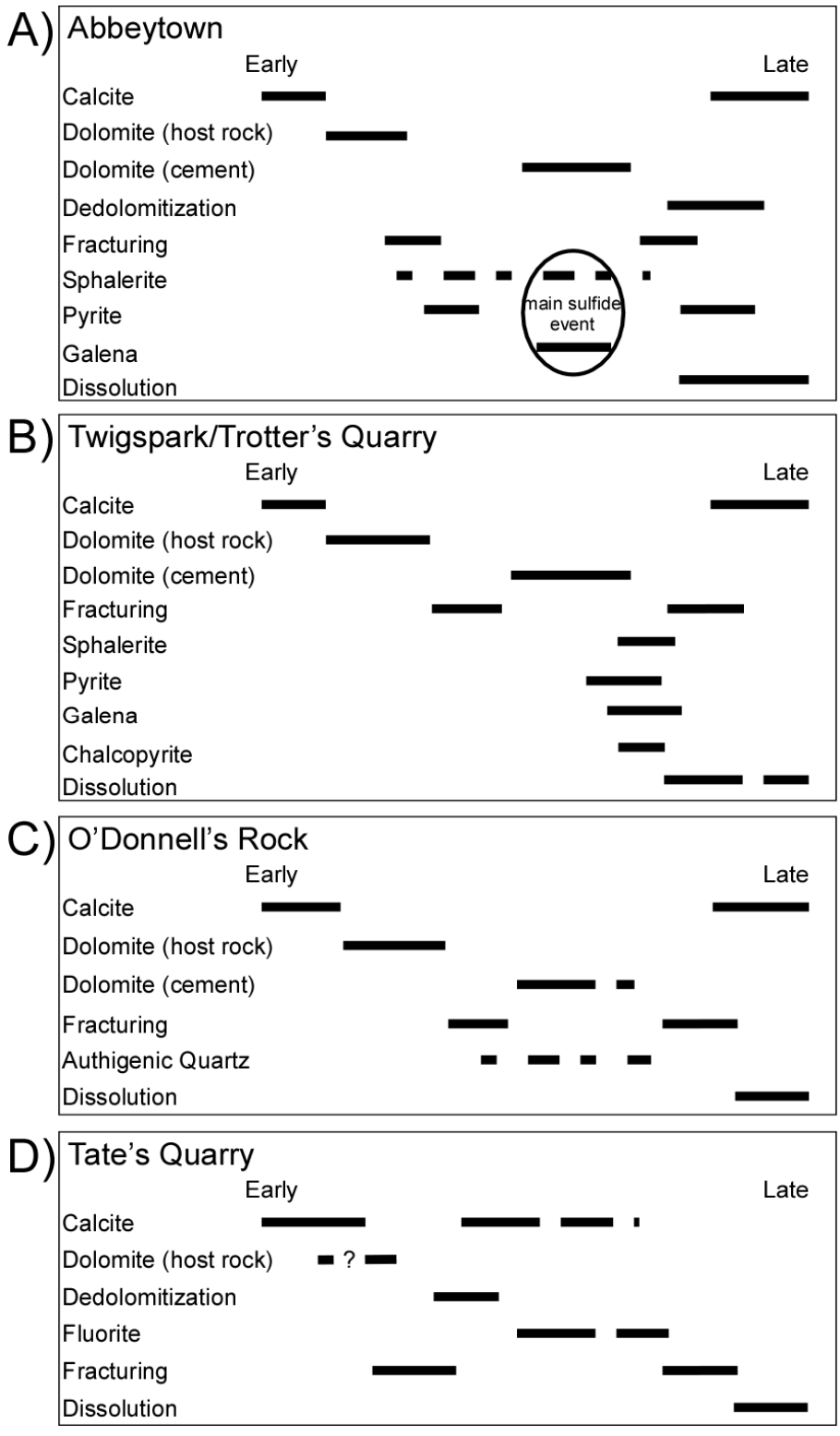

Figure 11. Paragenetic sequence of events for A) Abbeytown, B) Twigspark/Trotter's Quarry, C) O'Donnell's Rock, and D) Tate's Quarry. Note multiple sulfide mineralization events at Abbeytown compared to a single mineralization event at TWC/TQ.

Fluid Inclusions

Dolomite-hosted Inclusions

Measured inclusions in dolomite were 5-8 µm and rarely >8 µm in size. Smaller inclusions are common but were not measured due to poor resolution. Vapor bubble movement at room temperature was rare. At elevated (~80 °C) temperatures, bubble movement became apparent. Inclusions contained 2-5% vapor volume at 80 °C.

Homogenization temperatures (T_h) of inclusions in dolomite range from 105 to 207 °C with an average T_h value of 151 °C and a median of 145 °C (Fig. 12A). Frequency of T_h values displays a bimodal distribution across this range (Fig. 13A). Final ice-melting temperatures (T_m) range from -2.7 to -11.2°C, reflecting calculated salinities of 4.5 to 15.0 wt. % NaCl equivalent using the equations of Bodnar (1992). An average first-melt temperature (T_{fm}) of -31.6°C indicates the presence of other complex salts in addition to NaCl, such as $CaCl_2$ and KCl (Reynolds and Goldstein, 1994).

Inclusions from the Abbeytown main ore body plot as two populations, a lower temperature (108-147°C) - lower salinity (5-10 wt. % equiv. NaCl) population and a higher temperature (157-207°C) - higher salinity (9-15 wt. % equiv. NaCl) population (Fig. 12A). Inclusions from the western ore body plot as a single population, with T_h values reaching a maximum of 173°C and rarely exceed 160°C. Salinities of fluid inclusions from the western ore body occupy the same range of values as the two data populations in the main ore body fluid inclusions.

Sphalerite-hosted Inclusions

Measured inclusions were 3-6 µm in size. T_m values were not obtained for some smaller inclusions. Inclusions held a vapor volume of 2-5% at 20 °C. T_h values of these inclusions range from 109 to 168 °C with an average and median of 132°C (Fig. 12A). T_m values are evenly distributed across a range of -7.0 to -12.6 °C, corresponding to salinities of 10.5 to 16.5 wt. % equiv. NaCl (Bodnar, 1992). An average T_{fm} value of -32.5 °C was measured in sphalerite-hosted inclusions. Inclusions from the Index Bed are slightly less saline (by ~1 wt. % equiv. NaCl) than inclusions from beneath the Index Bed.

Calcite-hosted Inclusions

Inclusions ranged in size from 5 to 12 µm. Vapor volumes in calcite inclusions were consistently 2-5% at 20 °C. T_h values of inclusions in calcite range from 70 to 220 °C (Fig. 12A). T_h values over 190 °C are rare and may represent reequilibrated or stretched inclusions (Goldstein and Reynolds, 1994). T_m values range from -2.5 to -20.4 °C, corresponding to salinities of 4.2 to 22.7 wt. % equiv. NaCl. Salinities greater than 13 wt. % equiv. NaCl were observed in two samples: one from the western ore body and the other from within the Index Bed. T_{fm} values range from -22.3 to -42.3 °C, although temperatures below -30 °C are less common.

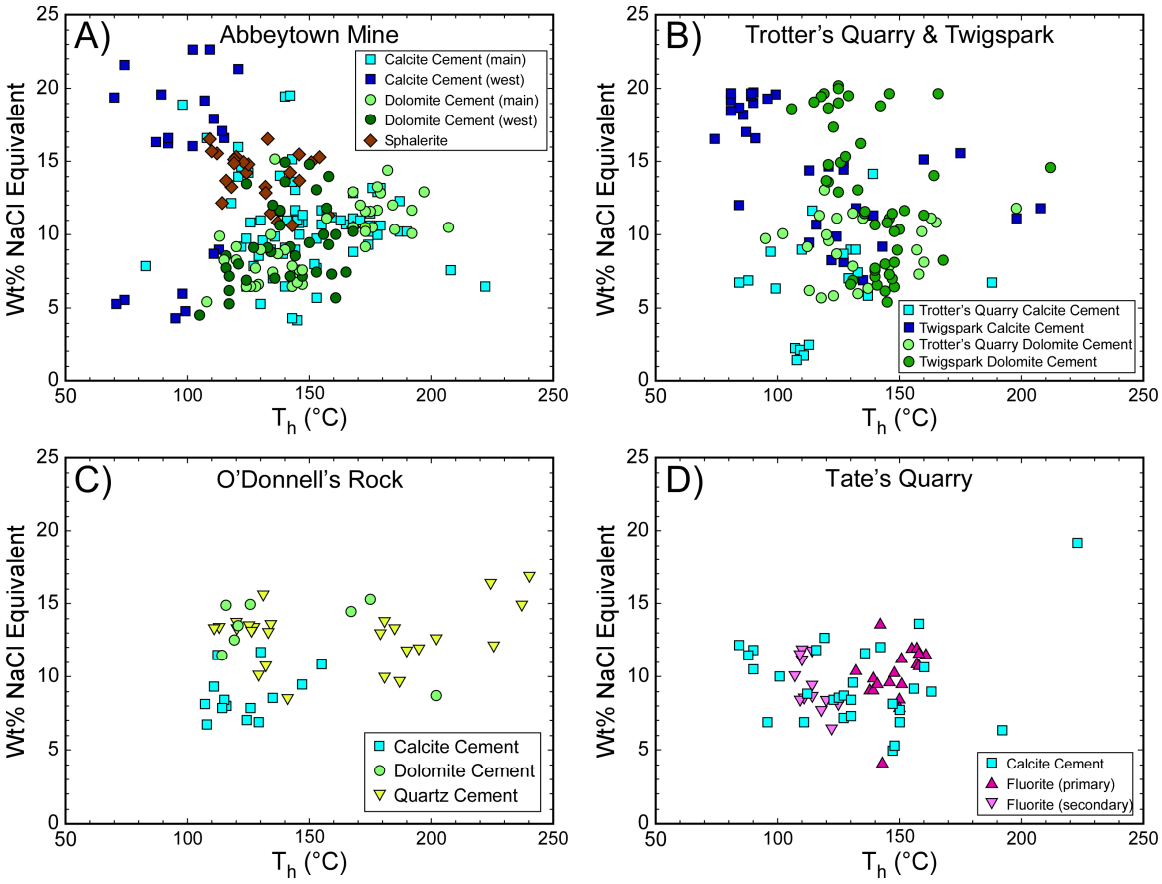

Figure 12. T_h values vs. wt. % equiv. NaCl for four localities in northwest Ireland. Salinities were calculated from T_m values according to equations from Bodnar (1992). Separate notations are used for calcite and dolomite fluid inclusions from the Abbeytown main and western ore bodies.

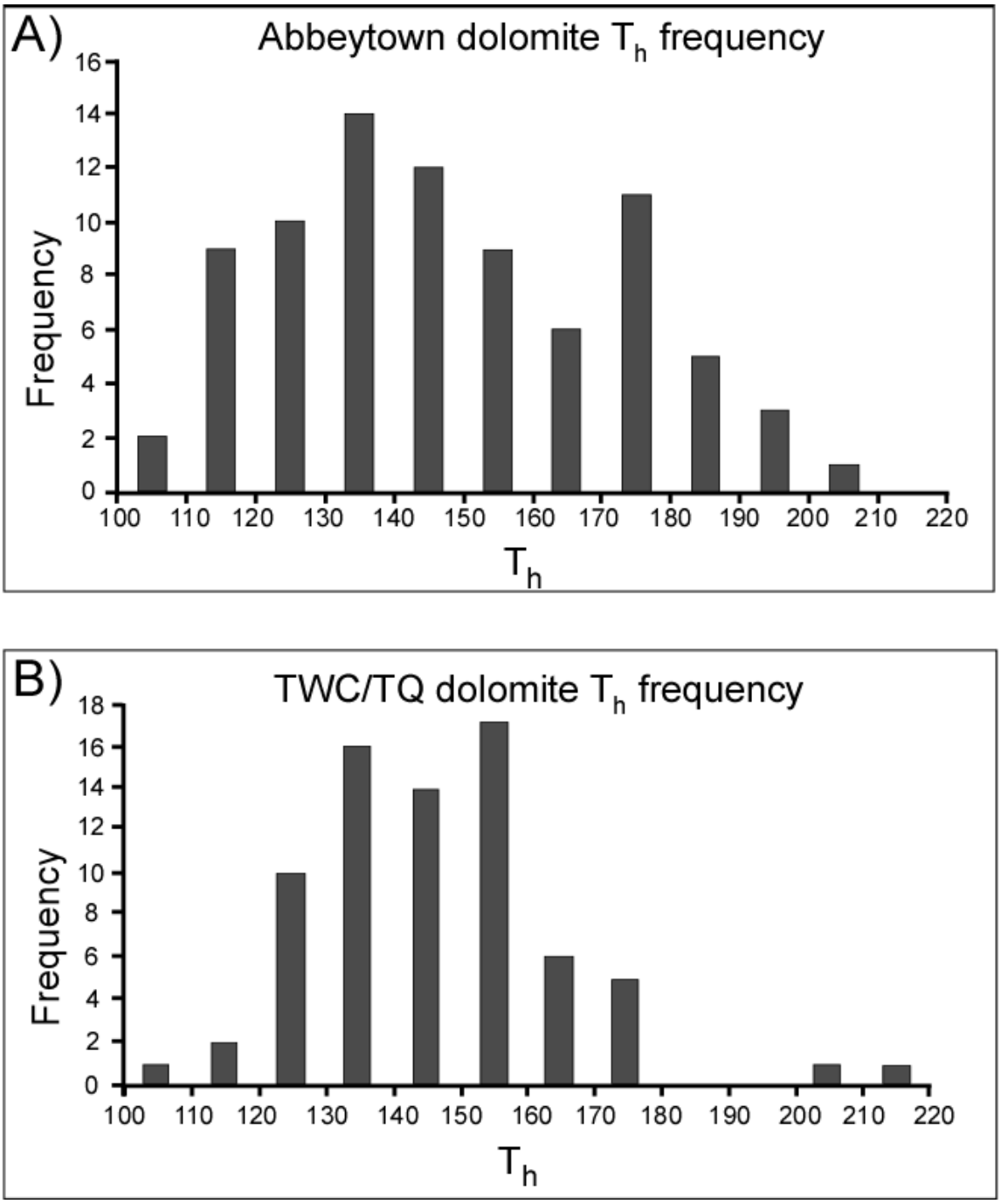

Figure 13. Histogram of T_h values in fluid inclusions in dolomite cements from A) Abbeytown and B) Twigspark/Trotter's Quarries and cores (TWC/TQ). Both localities display a bimodal distribution of data, although less evident in TWC/TQ T_h values.

Carbon and Oxygen Isotopes

Host limestones at Abbeytown Mine and Quarry display $\delta^{13}C$ values of 1.28 to 4.33‰ VPDB and $\delta^{18}O$ values of -8.98 to -6.56‰ VPDB (Fig. 14A). Host dolomites show $\delta^{13}C$ and $\delta^{18}O$ values of 2.07 to 4.07‰ and -9.86 to -8.19‰, respectively. Dolomite cements from the main ore body display $\delta^{13}C$ and $\delta^{18}O$ values of 3.36 to 3.60‰ and -7.40 to -5.39‰, respectively. Dolomite cements from the western ore body display lower $\delta^{13}C$ and $\delta^{18}O$ values of 2.11 to 2.99‰ and -10.92 to -8.57‰, respectively. Calcite cements display $\delta^{13}C$ and $\delta^{18}O$ values of 0.52 to 2.34‰ and -13.52 to -7.88‰, respectively.

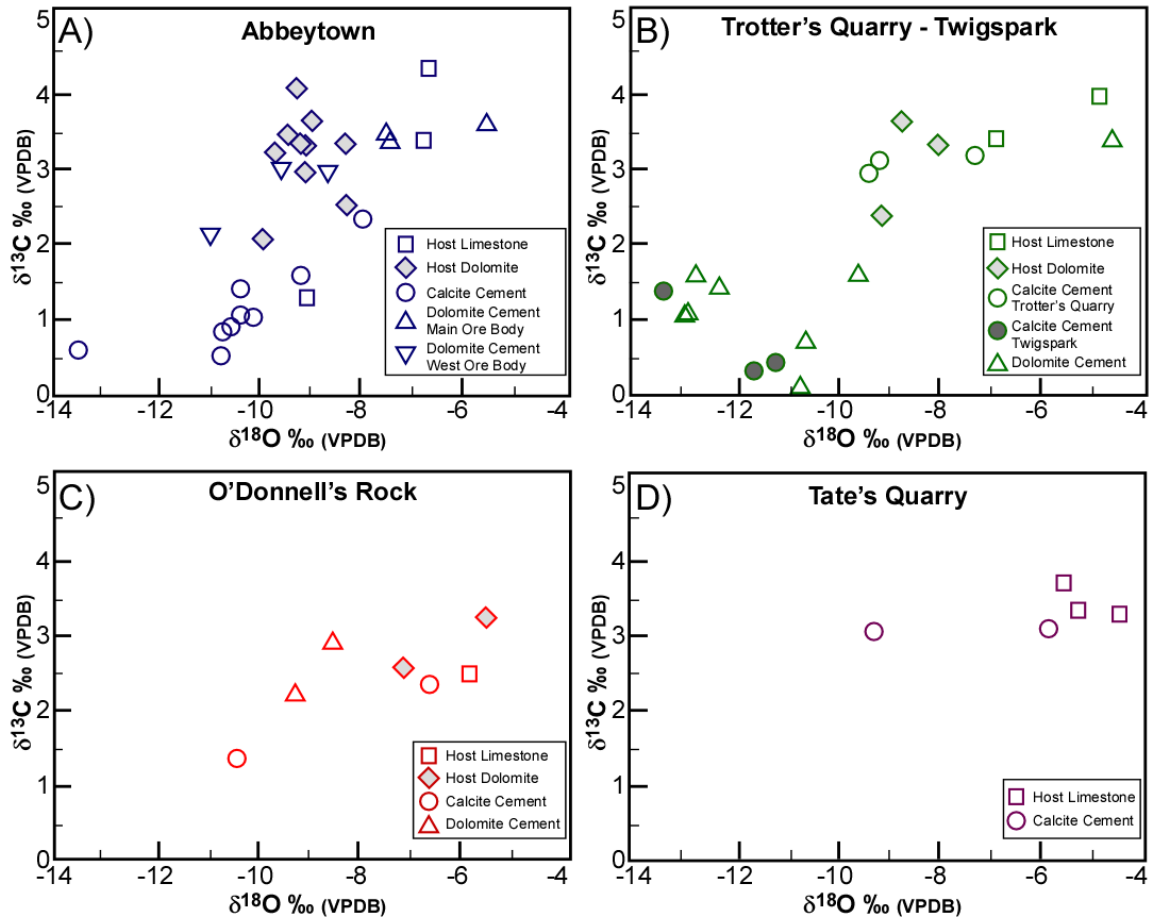

Figure 14. Plot of $\delta^{13}C$ ‰ vs. $\delta^{18}O$ ‰ values for the sampled localities in northwest Ireland.

Twigspark/Trotter's Quarries

Petrography

At Twigspark and the nearby Trotter's Quarry (TWC/TQ), carbonates were deposited as mud mounds draped by thin (< 1 m) shale beds. The Dartry Limestone, observed in surface quarries (Fig. 7D), is composed of primary micritic mud. Dolomitization of original limestone occurs sparsely at Trotter's Quarry and is more intense in the stratigraphically lower Twigspark Quarry and associated cores. Undolomitized limestone at Trotter's Quarry exhibits crypto-fibrous calcite (CFC), a possible neomorphic feature (Fig. 15 A-B) (Gregg *et al*., 2001). Stromatactis structures are present in mud mound cores and are commonly filled with calcite cement.

Detrital grains are abundant at Twigspark and are dominantly quartz with minor detrital alkali feldspars and micas. Abundance of detrital material increases down section. Original limestone at Twigspark is replaced commonly by dolomite. Replacement dolomite is coarsely crystalline (1-2 mm) planar-s dolomite, though planar-e and nonplanar dolomite are also present (Fig. 15 C-D).

Epigenetic carbonate cements occupy most fractures and vugs. Large (8-10 mm), saddle dolomite formed in fractures followed paragenetically by minor sulfide mineralization and blocky calcite cements. Pressure dissolution features are present in some samples. Uncemented fractures, dissolution of detrital grains (probably feldspars), and dissolution of saddle dolomite crystals account for the presence of significant porosity at Twigspark.

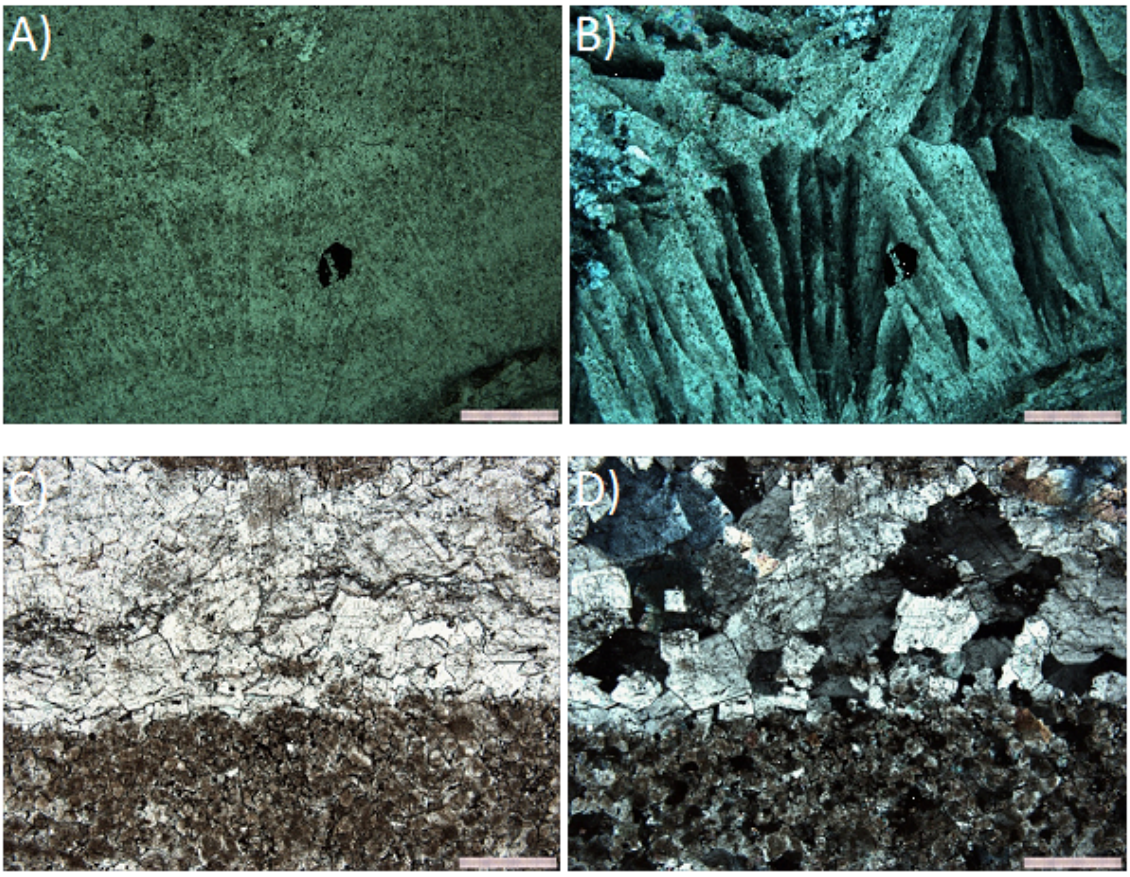

Figure 15. A) and B) PPL and XPL views of limestone from Trotter's Quarry showing crypto-fibrous calcite (CFC) [TQ-4]. Scale = 1 cm. C) and D) Dolomitized host rock (bottom) and dolomite cement (top) filling a vein in PPL and XPL views [TWC-3]. Scale = 1 cm.

Cathodoluminescence

Planar replacement dolomite crystals from the Twigspark cores exhibit a common CL microstratigraphy consisting of three zones: TZ1) a moderately luminescent, commonly mottled core, TZ2) a slightly darker, multi-banded zone, and TZ3) a brightly luminescent outer zone (Fig. 16 A-B). The thickness of zone 3 is consistent within each sample but varies between samples. This microstratigraphy is consistent and is correlated through >200 m of vertical section in borehole #TP96-3.

Epigenetic saddle dolomite cements from the Twigspark area display varying CL zonation patterns at different stratigraphic levels, however the outer zones correlate throughout the section. Present at all levels is a distinct two-zone CL pattern consisting of a wide, non-luminescent inner zone and a typically thin, brightly luminescent outer rim (Fig. 16 C-D).

Additional CL zones are present in the interior of dolomite cement crystals collected from Trotter's Quarry. As many as three additional zones are observed: i) a slightly luminescent to non-luminescent core, ii) a wide, moderately luminescent, mottled zone, and iii) a thin, slightly darker zone. In all occurrences, the common two-zone pattern observed in dolomite cement from the Twigspark area exists beyond zone [iii]. Zones [ii] and [iii] are present without zone [i] in one sample from the Twigspark cores, from a depth of 318 m (approx. 80 m above the contact with the basement rocks).

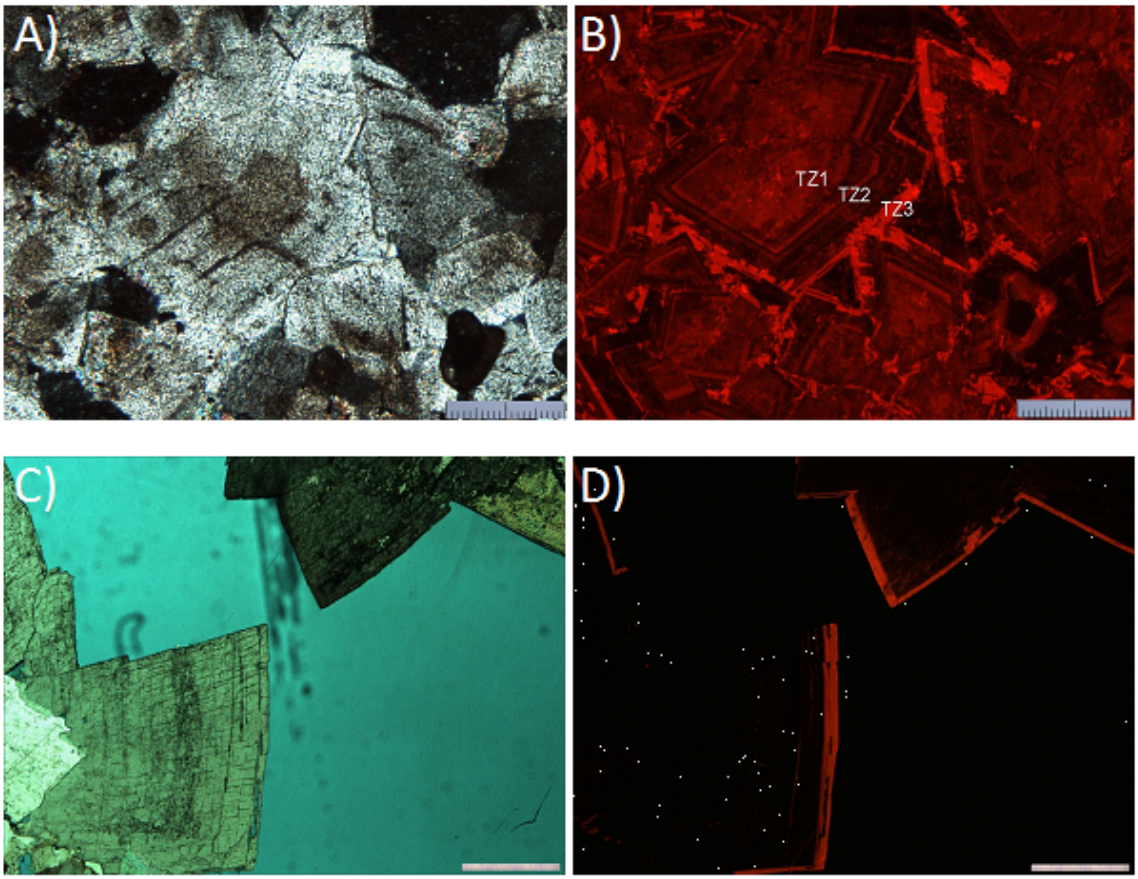

Figure 16. A) and B) XPL and CL photomicrographs of replacement dolomite from Twigspark. CL zones TZ1-3 are labeled [TWC-3]. Scale = 2 mm. C) and D) XPL and CL photomicrographs of common saddle dolomite cement [TWC-5]. Scale = 1 cm.

Paragenesis

Sedimentation in the TWC/TQ area first consisted of the deposition of carbonate mixed with siliciclastic material likely derived from local paleohighs associated with the uplift of the Ox Mountains Inlier. The contribution of detrital sediment decreased over time, allowing for carbonate production to dominate. Following burial, much of the section was dolomitized (Fig. 11B). Remaining fractures and vugs were filled by a single event of baroque dolomite cement. Minor sulfide mineralization comprising sphalerite, galena, pyrite, and chalcopyrite filled the remnant porosity. Pressure dissolution, observed in the form of horizontal stylolites, and a period of fracturing, followed dolomite and sulfide formation. The resulting fractures, when cemented, were filled by blocky calcite cements.

Fluid Inclusions

Dolomite-hosted Inclusions

Fluid inclusions in dolomite typically range in size from 4 µm to 8 µm. Vapor bubbles were undetectable at 20 °C. T_h values in dolomite range from 95 to 212 °C (Fig. 12B) with an average of 137 °C and a median of 136 °C. The frequency of T_h values is shown in Figure 13B. Salinities range from about 6 wt. % equiv. NaCl to over 20 wt. % equiv. NaCl (Fig. 12B). A majority of the inclusions measured were less than 12 wt. % equiv. NaCl. Salinities exceeding 15 wt. % equiv. NaCl were only observed in one core sample. T_{fm} values range from -21.3 to -49.2 °C. T_{fm} values below -30 °C are common. Three distinguishable growth zones were observed and fluid inclusions within each zone

were measured in one dolomite sample from the Twigspark cores. The measured variations between the three zones were small but the outermost growth zone is generally more cool and less saline (T_h avg. 140 °C; ~7 wt. % equiv. NaCl) than the innermost zone (T_h avg. 146 °C; ~9 wt. % equiv. NaCl). Under CL, these growth zones correspond to the common two-zone CL microstratigraphy seen in dolomite cement at Twigspark (see Fig. 16D).

Calcite-hosted Inclusions

Inclusion sizes range from 2 µm to >10 µm, but are commonly 5-8 µm. T_h values in calcite inclusions range from 74 to 208 °C (Fig. 12B). T_m values range from -0.8 to -16.4 °C, corresponding to salinities of 1.4 to 19.8 wt. % equiv. NaCl. T_{fm} values range from -22.7 to -44.2 °C and are typically > -33 °C.

When displayed together, the data define distinct populations. A lower temperature (T_h=74-99 °C), higher salinity (>16 wt. % NaCl) population (mostly Twigspark) and a slightly warmer (T_h=107-113 °C), lower salinity (<3 wt. % NaCl) population are evident. Remaining data plot between 5 and 15 wt. % equiv. NaCl with a large range of T_h values. The higher-salinity and lower-salinity data populations were each observed in only one sample. Both of these samples contained inclusions of the general population as well.

Carbon and Oxygen Isotopes

Host limestones from Twigspark cores and Twigspark and Trotter's quarries have $\delta^{13}C$ values of 3.40 to 3.96‰ and $\delta^{18}O$ values of -6.70 to -4.66‰ (Fig. 14B). Host

dolomites have $\delta^{13}C$ and $\delta^{18}O$ values of 2.37 to 3.62‰ and -8.97 to -7.86‰ respectively. Dolomite cements have $\delta^{13}C$ and $\delta^{18}O$ values of 0.10 to 1.59‰ and -12.89 to -9.45‰, respectively, excluding one datum ($\delta^{13}C$ = 3.38, $\delta^{18}O$ = -4.39). Values obtained from calcite cements plot as two separate populations. Calcite cements from Trotter's Quarry have $\delta^{13}C$ and $\delta^{18}O$ values of 2.95 to 3.18‰ and -9.22 to -7.12‰ respectively. Calcite from the Twigspark cores have lower $\delta^{13}C$ and $\delta^{18}O$ values of 0.32 to 1.37‰ and -13.32 to -11.08‰ respectively.

East of Ox Mountains Inlier – O'Donnell's Rock and Tate's Quarry

Petrography

Host limestone at O'Donnell's Rock is a fossiliferous grainstone and is commonly dolomitized in the sampled area. The lateral extent of dolomitization is unknown. Replacement dolomite is bimodal between medium crystalline (< 1 mm) planar-s to nonplanar and very coarsely crystalline (2-3 mm) planar-e rhombs. Epigenetic mineralization consists of vug- and fracture-filling calcite, dolomite and quartz, with an absence of sulfides. Dolomite cement consists of 5-10 mm saddle crystals. Void-filling calcite is blocky, 1-2 cm cement that becomes finer to the interior of vugs and fractures. Quartz cement is polymorphic crystalline with individual grains up to 1 cm in size. Fractures are filled primarily with calcite and trace quartz.

Limestone at Tate's Quarry is a fossiliferous grainstone and packstone, replaced infrequently by planar-e dolomite (< 10% volume), which has undergone minor dedolomitization. Epigenetic dolomite cement and sulfide mineralization is absent from this location. Void-filling cements consist primarily of blocky calcite with trace amounts of fluorite.

Cathodoluminescence

Planar-s and nonplanar replacement dolomite at O'Donnell's Rock are moderately luminescent and display no zoning under CL (Fig. 17 A-B). Planar-e replacement dolomite exhibits a simple two-zone pattern with a luminescent core and an outer band of moderate CL with a similar appearance to the unzoned dolomite. Rhombs of dolomite

cement display a two-zone pattern consisting of a moderately luminescent core with a thin nonluminescent outer rim.

Replacement dolomite at Tate's Quarry exhibits a two-zoned microstratigraphy consisting of a mottled core with a thin, brightly luminescent outer rim (Fig. 17 C-D). In one sample, two additional CL bands are present beyond the outer rim. The additional zones consist of a nonluminescent band followed by an outer brightly luminescent band. Fluorite crystals emit a homogeneous blue CL with no zoning.

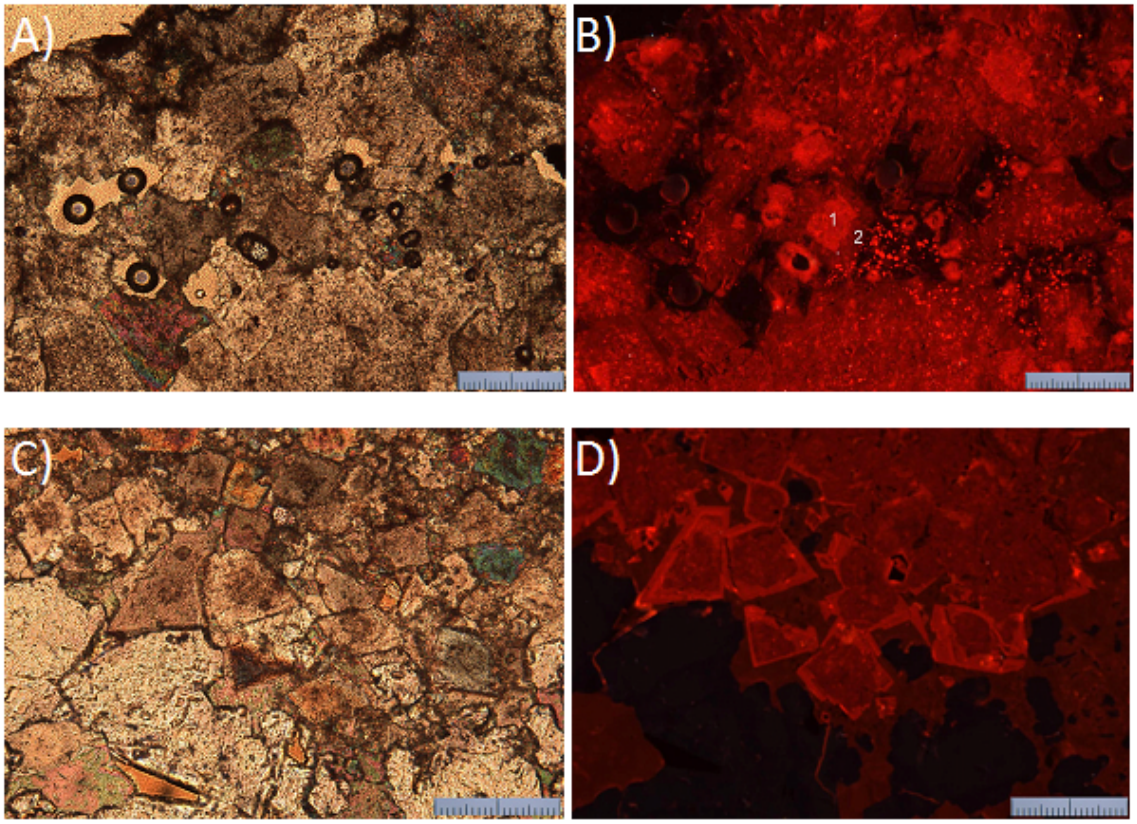

Figure 17. A) and B) XPL and CL photomicrographs of replacement dolomite from O'Donnell's Rock [OR-1]. Two-zoned planar-e dolomite is labeled. Note nonplanar, unzoned dolomite along bottom of picture. Scale = 2 mm. C) and D) XPL and CL photomicrographs of replacement dolomite from Tate's Quarry [TAQ-1]. Dark luminescence is fluorite. Scale = 2 mm.

Paragenesis

At O'Donnell's Rock original fossiliferous limestone was partially replaced by dolomite (Fig. 11C). Following initial dolomitization and a period of fracturing, authigenic quartz and dolomite were precipitated in open spaces. Calcite mineralization during this period is present but minor. A later period of fracturing preceded late diagenetic calcite precipitation. Post-cementation dissolution has resulted in the formation of secondary porosity. At Tate's Quarry, original limestone and early marine cementation underwent minor dolomitization (Fig. 11D). Following a period of fracturing, calcite and fluorite filled resulting fractures and remaining porosity. Minor dedolomitization was observed at Tate's Quarry.

Fluid Inclusions

Dolomite-hosted Inclusions

Inclusion sizes in dolomite at O'Donnell's Rock were 2-4 µm. Vapor content was undetectable at 20 °C, but content ranged 1-5% at elevated (80-90 °C). T_h values for inclusions in dolomite at O'Donnell's Rock range from 114 to 202 °C with an average of 143 °C (Fig. 12C). T_m values range from -5.6 to -11.3 °C, corresponding to salinities of 8.7 to 15.3 wt. % equiv. NaCl. T_{fm} values range from -34.4 to -50.6 °C.

Calcite-hosted Inclusions

Inclusions in calcite from O'Donnell's Rock were 2-6 µm in size with a vapor content of 2-5 volume %. T_h values range from 107 to 130 °C, rarely extending to a

maximum of 155 °C (Fig. 12C). The average T_h was 124 °C. T_m values range from -4.2 to -8.0 °C, corresponding to salinities of 6.7 to 11.7 wt. % equiv. NaCl, with an average of 8.7 wt. % equiv. NaCl. T_{fm} values were not measured for all inclusions, but when obtained, range from -30.8 to -48.6 °C.

Inclusions in calcite from Tate's Quarry were typically 4-6 µm in size with a vapor content of 2-5 volume %. T_h values range from 84 to 223 °C (Fig. 12D). T_h>165 °C are rare and may be regarded as anomalies. Ignoring these data, the range of T_h values is 84 to 163 °C, with an average temperature of 116 °C and median of 127 °C. T_m values range from -3.0 to -9.7 °C, corresponding to salinities of 5.0 to 13.6 wt. % equiv. NaCl. T_{fm} values range from -21.5 to -35.0 °C.

Quartz-hosted Inclusions

Fluid inclusions in quartz from O'Donnell's Rock were 4-10 µm in size. Vapor content ranged from 1 to 10 volume %. T_h values range from 111 to 240 °C (Fig. 12C). Two clusters of data are present, a lower temperature (111-149 °C) group and a higher temperature (179-240 °C) group. T_m values range from -5.4 to -12.8 °C, corresponding to salinities of 8.4 to 16.7 wt. % equiv. NaCl. Salinities are consistent across both T_h populations.

Fluorite-hosted Inclusions

Fluid inclusions in fluorite from Tate's Quarry range in size from 4 to 10 µm. The vapor content of these inclusions was commonly 5 volume %. Primary and secondary fluid inclusions are observed in fluorite. T_h values of primary inclusions range

from 132 to 161 °C with an average of 148 °C (Fig. 12D). T_h values of secondary inclusions range from 107 to 125°C with an average T_h value of 114°C. T_m values do not vary between primary and secondary inclusions and range from -2.5 to -9.8 °C, corresponding to salinities of 4.2 to 13.7 wt. % equiv. NaCl. T_{fm} values range from -19.6 to -30.0 °C.

Carbon and Oxygen Isotopes

A single sample of host limestone at O'Donnell's Rock has a $\delta^{13}C$ value of 2.47‰ and a $\delta^{18}O$ value of -5.74‰ (Fig. 14C). Host dolomites have $\delta^{13}C$ and $\delta^{18}O$ values of 2.57 to 3.23‰ and -7.06 to -5.41‰ respectively. Dolomite cements have $\delta^{13}C$ and $\delta^{18}O$ values of 2.20 to 2.88‰ and -9.20 to -8.45‰ respectively. Calcite cements have $\delta^{13}C$ and $\delta^{18}O$ values of 1.35 to 2.33‰ and -10.37 to -6.55‰ respectively.

Host limestone samples from Tate's Quarry have $\delta^{13}C$ and $\delta^{18}O$ values of 3.27 to 3.68‰ and -5.35 to -4.26‰ respectively (Fig. 14D). Calcite cements have $\delta^{13}C$ and $\delta^{18}O$ values of 3.03 to 3.037 and -9.15 to -5.66‰ respectively.

CHAPTER V

DISCUSSION

Sedimentation and early diagenesis

Field relationships coupled with the relatively homogeneous $\delta^{13}C$ and $\delta^{18}O$ values measured in host limestones and similar petrographies from the four study localities suggest marine sedimentation conditions were similar across the region. This is supported by facies distribution mapping conducted by Cózar *et al*. (2005) and Somerville *et al*. (in prep.). The range of $\delta^{13}C$ values in northwest Ireland marine limestones are similar to values from the Courceyan-Chadian Waulsortian Limestone in the Irish Midlands (Gregg *et al*., 2001); however the Waulsortian Limestone displayed slightly higher $\delta^{18}O$ values (0.0 to -4.0‰ PDB). The $\delta^{13}C$ and $\delta^{18}O$ values obtained from northwest Ireland are a good match for limestone deposited from typical Lower Carboniferous seawater (Popp *et al*., 1986).

Relatively homogeneous sedimentary deposition throughout the northwest Ireland region suggests that uplift of the Ox Mountains Inlier occurred after sedimentation. Hitzman (1986) proposed that the Ox Mountains were not a paleogeographic feature at the onset of marine deposition during the Chadian due to the absence of coarse clastics at the base of the sedimentary strata; however pebbly channels within the Ballyshannon Limestone suggest movement of faults may have begun in the late Chadian or early

Arundian. Somerville *et al.* (in prep.) observed facies thickness variations in Glencar and Dartry Limestone strata, suggesting significant uplift had occurred prior to the early Asbian. Stratigraphy and isotope geochemistry indicate that uplift of the Inlier did not affect carbonate sedimentation.

Although limestone formation appears sedimentologically and geochemically consistent across northwest Ireland, the influence of structural features on early diagenetic processes is evident. Host dolomite's $\delta^{13}C$ and $\delta^{18}O$ values display a tight cluster between samples from Abbeytown and those from Twigspark and Trotter's Quarries (TWC/TQ) (Fig. 14). This indicates that early dolomitization processes likely were consistent between the two areas. Host dolomite from O'Donnell's Rock has $\delta^{18}O$ values more positive than those measured at Abbeytown or TWC/TQ possibly indicating dolomitizing fluids derived from a different source at sample locations east of the Ox Mountains Inlier.

CL microstratigraphies of host dolomite can be traced within individual sample localities but do not correlate among the four localities within the northwest Ireland region. Differences in host dolomite CL microstratigraphies are largest between eastern and western locations, suggesting that structural isolation, resulting in a lack of a regionally extensive paragenetic sequence, may have already been attained prior to host rock dolomitization.

Characterization of mineralizing fluids

Occurrences of mineralization in northwest Ireland are related closely to major structural features in the region and appear to be isolated structurally from one another.

Both Abbeytown and TWC/TQ are located in close proximity to the Ox Mountains-Pettigoe Fault (OMPF), a regional structural feature associated with the uplift of the Ox Mountains (Fig. 2). Tate's Quarry and O'Donnell's Rock are in the vicinity of the Dromahair Fault, a companion fault to the OMPF that defines the southern and eastern edge of the uplift. Locally, the distribution of mineralization at Abbeytown is observed to be dependent on the presence of structural features including the Abbeytown Fault, a high-angle reverse fault (Fig. 3).

Paragenetic sequences determined by petrographic analysis of the four sampled localities further illustrate the lack of regionally persistent diagenetic events (Fig. 11A-D). Sulfide mineralization at Abbeytown occurred in multiple phases, an early sphalerite and pyrite phase, followed by the main sphalerite and galena phase punctuated by a relatively late pyrite phase (Fig. 11A). Two observed stages of dolomitization at Abbeytown are likely related to two separate sulfide mineralization events. At TWC/TQ a single, paragenetically late sulfide event is observed that accounts for all Pb-Zn-Fe mineralization observed (Fig. 11B). However, multiple stages of dolomitization are also observed at this locality. The eastern localities, Tate's Quarry and O'Donnell's Rock, contain no known sulfide mineralization. Instead, each locality has a unique paragenetic sequence with diverse mineralogy.

In northwest Ireland there is an absence of a regionally correlative dolomite CL microstratigraphy such as that observed in the Irish Midlands mineral district (Gregg *et al*., 2001; Wright *et al*., 2001; and Wright, 2002). CL microstratigraphies in dolomite host rock and dolomite cements at Abbeytown are correlative stratigraphically and laterally between the main and western ore bodies (Z1-Z4 and CZ1-CZ4 zones,

respectively), indicating that a common set of fluids was present throughout that area (Fig. 10 A-F). Dolomite CL microstratigraphies at TWC/TQ correlate well in both quarries and stratigraphically in the associated cores, but do not correlate with the CL stratigraphies present at Abbeytown (Fig. 16 A-D) despite the observation that 3 zones are recognized. This indicates that the fluids that precipitated the epigenetic cements at TWC/TQ are unrelated to those observed at Abbeytown. CL microstratigraphies observed at O'Donnell's Rock and Tate's Quarry are somewhat similar to each other, but are significantly different from those observed at Abbeytown and TWC/TQ (Fig. 17 A-D). The presence of distinct CL stratigraphies in dolomite cements at each study location strongly indicates either geochemical evolution of regional mineralizing fluids (geographically or chronologically) or multiple, isolated fluid flow events.

Fluid evolution

Stable isotope ratios of carbonate cements are controlled by the isotopic composition of the formation fluids and the temperature of mineral precipitation. The isotopic composition of formation fluids can be calculated from T_h and $\delta^{18}O$ values of carbonate cements (Woronick and Land, 1985) to determine if the difference between measured $\delta^{18}O$ values in northwest Ireland (Fig. 14 A-D) is caused by a temperature effect, a fluid chemistry effect, or both. Dolomite cements from Abbeytown's main ore body, with an average T_h value of 159 °C, indicate a fluid with a $\delta^{18}O$ value of 10.1‰ SMOW (Table 1) while dolomite cements at the western ore body, with an average T_h value of 140 °C, suggest a fluid with a $\delta^{18}O$ value of 5.5‰ SMOW. These values are exactly opposite what should be expected if isotope variations were due to heating of a

single fluid. Twigspark and O'Donnell's Rock dolomite cements have average T_h values similar to the Abbeytown western ore body of 137 °C and 143 °C, respectively. These temperatures suggest fluids with $\delta^{18}O$ values of 3.2‰ and 7.0‰ SMOW at Twigspark and O'Donnell's Rock, respectively (Table 1). If measured $\delta^{18}O$ values were the result of heating of a regional fluid, the dolomite cements from warmer localities, such as the Abbeytown main ore body and O'Donnell's Rock, should indicate formation from isotopically lighter fluids than dolomite cements from cooler localities, such as the Abbeytown western ore body and TWC/TQ. The separation of groups of isotope data in northwest Ireland cannot be explained as a temperature variation of a single, regionally persistent fluid, such as that proposed by Hitzman (1986). Instead there must be a geochemical difference in fluids, either in the fluid source or exposure to different equilibrating rocks.

The distribution of $\delta^{18}O$ values from Abbeytown, TWC/TQ and O'Donnell's Rock could alternatively be accounted for in a single, regional fluid system if lower $\delta^{18}O$ values correspond to the presence of a meteoric water component. If meteoric water had an impact on fluids precipitating cements, there should be a measurable salinity difference in fluid inclusions between isotopically lighter dolomite cements from O'Donnell's Rock and the Abbeytown western ore body compared to cements from the Abbeytown main ore body. Salinities calculated from fluid inclusions in dolomite cements are instead relatively constant between the main and western ore bodies at Abbeytown and at O'Donnell's Rock (Table 2). A similar explanation could be offered to justify the $\delta^{18}O$ difference between calcite cements from Trotter's Quarry and those from the stratigraphically lower Twigspark Quarry cores, with the lower $\delta^{18}O$ calcite

cements from the Twigspark cores containing a larger component of meteoric water. Instead salinities calculated from fluid inclusions in calcite from the Twigspark cores are more saline (7 to 20 wt. % NaCl) than fluid inclusions from Trotter's Quarry calcite cements (1 to 9 wt. % NaCl) (Table 2). The salinity values are exactly opposite what would be expected if a regional fluid was mixing variably with meteoric water. Fluid inclusion evidence from calcite and dolomite cements at Abbeytown, TWC/TQ and O'Donnell's Rock alternatively suggest that a viable explanation for the observed variations in stable isotope values is that each locality was exposed to different sets of multiple, distinct fluids, which may have mixed variably.

Evaluation of fluid inclusion data at each of the four study localities may shed light on the genesis of sulfide mineralization in northwest Ireland. Figure 18A displays fluid inclusion data from calcite and dolomite cements and sphalerite from mineralization at Abbeytown. These data are interpreted to indicate the presence and mixing of three geochemically distinct end-member fluid types. Fluid type 1 (Ft1) is a lower temperature (T_h = 70-150 °C), lower salinity (4 to 9 wt. % NaCl) fluid; fluid type 2 (Ft2) is a lower temperature (T_h = 70-140 °C), higher salinity (15 to 24 wt. % NaCl) fluid; and fluid type 3 (Ft3) is a higher temperature (T_h = 165-220 °C), moderate salinity (8-14 wt. % NaCl) fluid (Fig. 18). It is not uncommon for more than one fluid type to be present in an individual calcite or dolomite cement crystal.

Involvement of three end-member fluids with similar T_h values and salinities as seen at Abbeytown is also observed at TWC/TQ (Fig. 18B). At TWC/TQ, a fluid with characteristics of Ft1 is only present in samples from Trotter's Quarry while an Ft2 fluid is present predominantly in stratigraphically lower intervals sampled from the Twigspark

cores (Fig. 18B). An Ft3 fluid is less well-developed than at Abbeytown as indicated by the paucity of inclusions with T_h values >170 °C.

Complex three-fluid trends were not observed in carbonate cements at either O'Donnell's Rock or Tate's Quarry (Fig. 18C & D). A fluid with characteristics similar to Ft3 is well developed at O'Donnell's Rock with T_h values >200 °C in authigenic quartz and, to a lesser extent, in dolomite cements. An Ft2-like fluid is absent. Fluid inclusions in calcite cements may indicate the presence of a fluid similar to Ft1, although the range of data displays higher T_h values and higher salinities (110 to 140 °C and 6 to 9 wt. % NaCl) at O'Donnell's Rock than at either Abbeytown or TWC/TQ.

At Tate's Quarry, both calcite- and fluorite-hosted fluid inclusions have similar T_h and T_m values (Fig. 18D). Inclusions in calcite at Tate's Quarry appear to be similar to those in calcite from O'Donnell's Rock, however it cannot be determined from fluid inclusion data alone whether or not the fluid at Tate's Quarry is equivalent to Ft1 at O'Donnell's Rock, a cooled Ft3-like fluid from O'Donnell's Rock, or a third, unrelated fluid. Calcite cement $\delta^{13}C$ and $\delta^{18}O$ values from O'Donnell's Rock and Tate's Quarry are similar, suggesting the same fluid may have affected the two geographically proximal locations.

Dolomite Cements	Average T_h (T_h range)	Average $\delta^{18}O$ (cem.)	Calculated $\delta^{18}O$ (water) (Calc. values for T_h range)
Abbeytown (main)	159 °C (108-207 °C)	-6.71‰ PDB	10.1‰ SMOW (5.2-13.4‰ SMOW)
Abbeytown (west)	140 °C (105-173 °C)	-9.66‰ PDB	5.5‰ SMOW (1.8-8.1‰ SMOW)
Twigspark	137 °C (95-212 °C)	-11.59‰ PDB	3.2‰ SMOW (-1.4-8.6‰ SMOW)
O'Donnell's Rock	143 °C (114-202 °C)	-8.45‰ PDB	7.0‰ SMOW (4.1-11.3‰ SMOW)

Table 1. Average T_h and $\delta^{18}O$ values of dolomite cements in northwest Ireland, and calculated $\delta^{18}O$ values in SMOW of formation fluids, using equations from Woronick and Land (1985).

Dolomite Cements	Average wt. % equiv. NaCl	Average $\delta^{18}O$ (cem.)
Abbeytown (main)	10.2	-6.71‰ PDB
Abbeytown (west)	9.5	-9.66‰ PDB
Twigspark	11.5	-11.59‰ PDB
O'Donnell's Rock	9.6	-8.83‰ PDB
Calcite Cements	**Average wt. % equiv. NaCl**	**Average $\delta^{18}O$ (cem.)**
Abbeytown (main)	10.8	-10.45‰ PDB
Abbeytown (west)	14.3	-10.09‰ PDB
Twigspark	14.7	-11.97‰ PDB
Trotter's Quarry	6.7	-8.45‰ PDB
O'Donnell's Rock	8.7	-8.46‰ PDB
Tate's Quarry	10.0	-7.41‰ PDB

Table 2. Average calculated salinities of dolomite and calcite cements from fluid inclusion T_m values (using equations from Bodnar, 1992) and average $\delta^{18}O$ values.

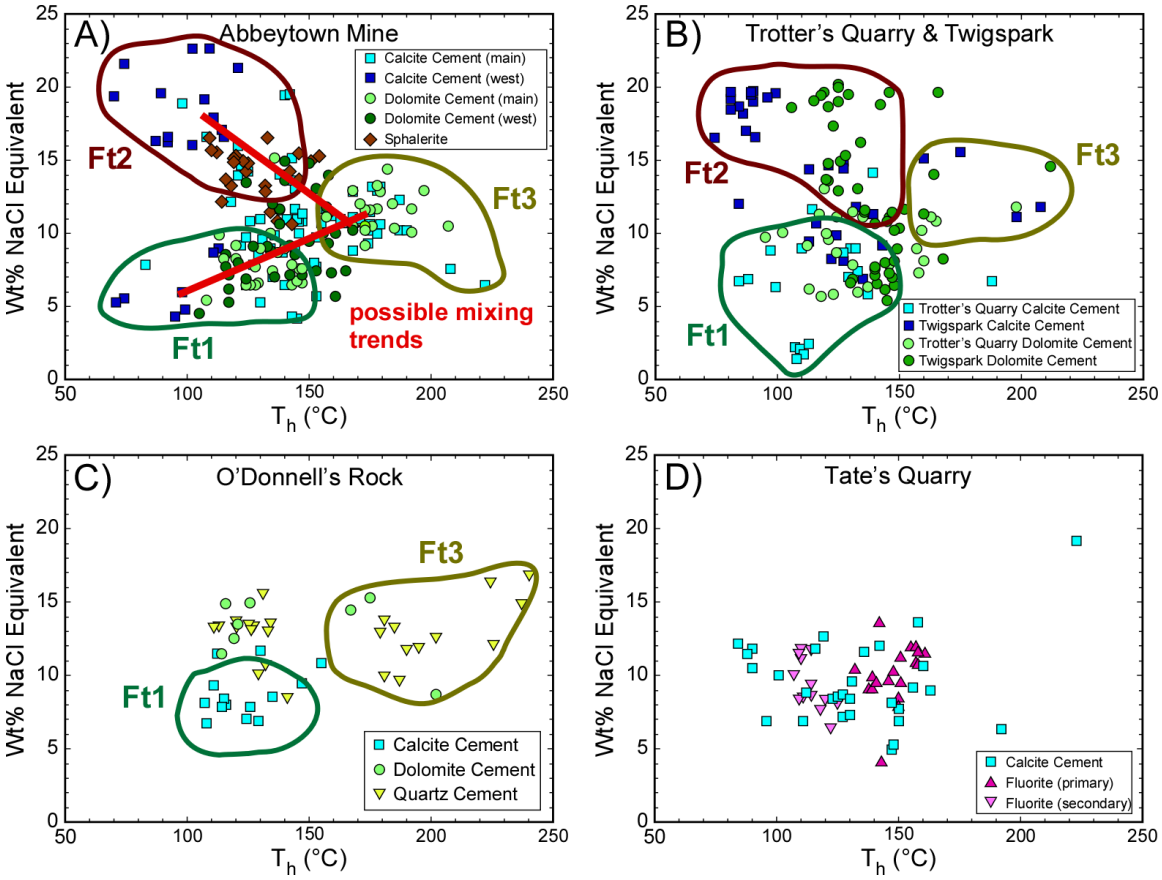

Figure 18. T_h vs. wt. % equiv. NaCl from four sampled localities in northwest Ireland with fluid types Ft1, Ft2, and Ft3 labeled. Possible fluid mixing trends at Abbeytown are indicated.

Origin and timing of mineralizing fluids

Fluid inclusion and geochemical studies conducted in the Irish Midlands on Waulsortian Limestone-hosted Pb-Zn deposits indicate the presence of three geochemically distinct fluids in the region. Banks *et al*. (2002) used halogen geochemistry of fluid inclusions to illustrate that the mixing of two end member fluids, one of which was evaporated seawater, was responsible for sulfide mineralization at the Tynagh and Silvermines deposits (Fig. 1). Wilkinson and Earls (2000), Wright *et al*. (2004), Wilkinson *et al*. (2005), and Johnson *et al*. (in press) all provide similar fluid inclusion and halogen geochemical evidence suggesting the presence of as many as three fluids during epigenetic dolomitization and mineralization in the Irish Midlands. Ore fluids in the Irish Midlands are believed to be seawater evaporated to high salinities, but not to the point of halite precipitation, that has leached metal ions from interactions with basement rocks (Wilkinson *et al*., 2005). This fluid mixed with seawater evaporated beyond the point of halite precipitation, which was rich in reduced sulfur.

In northwest Ireland, a similar regional fluid system is not indicated. However, three fluid types can be invoked. A higher-salinity fluid, Ft2, is present only at Abbeytown and TWC/TQ and may be analogous to the fluid described by Johnson *et al*. (in press) in the Irish Midlands as seawater evaporated beyond the point of halite precipitation. The presence of gypsum beds in the late-Asbian/Brigantian Meenymore Formation (Fig. 5) suggests evaporitic conditions were present within the basin after the deposition of the host limestones (Philcox *et al*., 1992; Cózar *et al*., 2005, 2006; Somerville et al., in prep.). Salinities calculated from fluid inclusion T_m values indicate

that in northwest Ireland this fluid is not evaporated beyond the point of halite precipitation, as it is in the Irish Midlands.

Ft1 and Ft3 fluids in northwest Ireland display similar characteristics as two of the fluid types from the Irish Midlands (Johnson *et al*., in press). The latter are fluids derived from modified seawater that circulated through basement rocks. The temperature difference between Ft1 and Ft3 in northwest Ireland may represent either a cooling trend or differences in the depths of penetration along faults and fractures of two different fluids; the higher T_h values of Ft3 would indicate deeper circulation and possible basement interaction. At Trotter's Quarry, Ft1 circulated into the Dartry Limestone but was not observed in underlying strata of the Twigspark and Ballyshannon Limestone formations sampled from the Twigspark cores. This indicates that these strata were not affected by this fluid or that cements were not precipitated containing this fluid type.

Fluid inclusions in sphalerite from Abbeytown form a cluster exclusively on a proposed mixing trend between Ft2 and Ft3 (Fig. 18A). The distribution of this data indicates that, as has been shown in the Irish Midlands, the interaction of evaporated seawater (Ft2) and a higher temperature fluid with possible basement interaction (Ft3) is required for sulfide ore mineralization (Wilkinson *et al*., 2005; Johnson *et al*., in press). Ft3 is poorly represented in fluid inclusions measured in epigenetic cements at TWC/TQ. This may be due to either a lesser developed or less abundant Ft3 fluid at TWC/TQ than at Abbeytown. The lack of a well-developed, higher-temperature fluid may be responsible for less abundant sulfide mineralization at Twigspark Quarry. At Abbeytown, the higher-temperature, moderate-salinity fluid may have penetrated downward along faults and fractures through basement rocks where it leached metal ions

before convecting upward, where it mixed with a sulfate-carrying brine, in a system similar to the thermohaline convection model proposed by Russell (1978) (Fig. 19).

There is no indication of the relative timing of mineralization at Abbeytown compared to TWC/TQ or the other localities studied, as no regionally consistent mineral paragenesis was observed. Hitzman (1986) suggested an Asbian or later timing for mineralization at Abbeytown. Dolomite CL microstratigraphies at TWC/TQ are correlated throughout the stratigraphic section suggesting dolomitization associated with mineralization at TWC/TQ occurred after deposition of the Dartry Limestone. This indicates the late Asbian as the earliest possible timing for the initiation of mineralization at TWC/TQ. At both localities mineralization is shown to have taken place after the initial onset of movement of faults associated with uplift of the Ox Mountains Inlier. The relative timing of mineralization compared with later reactivation of basement faults in the Late Carboniferous is undetermined.

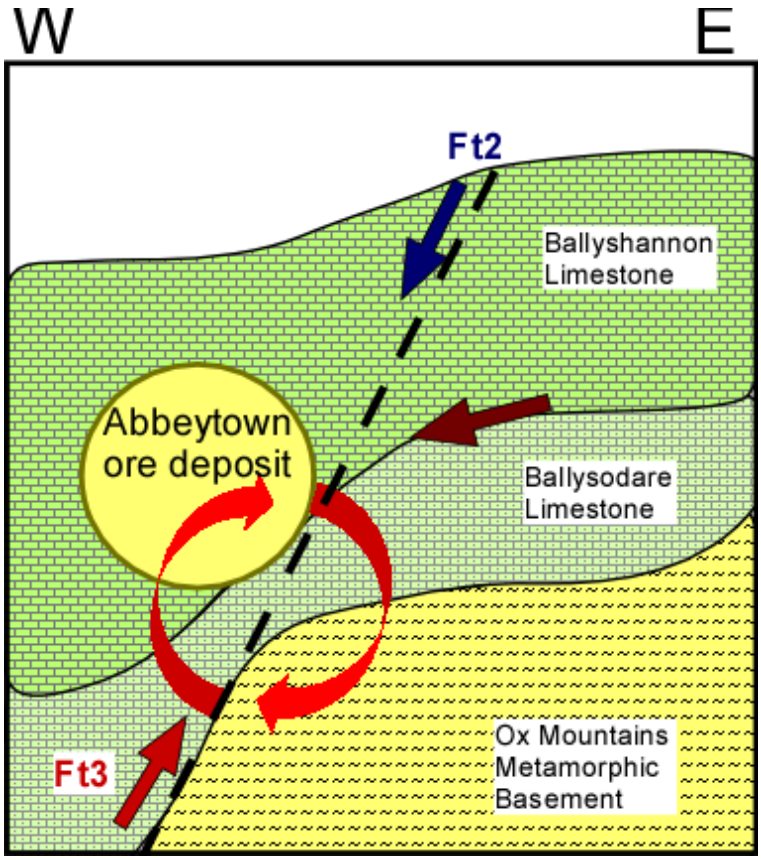

Figure 19. Proposed fluid convection/mixing model at Abbeytown Mine. Ft3 migrates down faults, leaches metal ions from basement metasedimentary rocks, migrates upward following heating and mixes with Ft2. Modified from Johnson *et al*. (in press).

Comparison to mineralization in the Rathdowney Trend, Irish Midlands

Mineralization in northwest Ireland represents a separate system, isolated geologically from the Pb-Zn district in the Rathdowney Trend and the Irish Midlands (Fig 1). Circulating fluids in northwest Ireland likely interacted with Precambrian metasedimentary basement rocks while the basement in the Irish Midlands consists of Silurian-Devonian volcanic and metasedimentary rocks. Additionally, the absence of a thick basal Devonian or Lower Carboniferous siliciclastic formation in the Sligo Syncline of northwest Ireland likely had an impact on the fluid system of the area. The Devonian Old Red Sandstone in the Irish Midlands may have served as a conduit for regional fluid flow, if not also acting as a source of metal ions for mineralization (Hitzman and Beaty, 1996; Hitzman *et al*., 1998; Wright *et al*., 2003; Johnson *et al*., in press). There is an absence of an underlying siliciclastic formation, similar to the Old Red Sandstone, in northwest Ireland. No such regional fluid flow system is indicated by this study for the Sligo Syncline.

Synsedimentary faulting as a result of the uplift of the Ox Mountains Inlier has been shown to have had significant effects on distribution of Carboniferous sedimentary facies in northwest Ireland, especially in the Visean (Hitzman, 1986; Cózar *et al*., 2005; Somerville *et al*., in prep.). Structural activity associated with uplift of the Inlier has also been shown to predate host rock dolomitization at all four mineralized locations. Structural movement in northwest Ireland likely disrupted any regional fluid system connectivity and promoted development of structurally isolated fluid circulation cells within the basin. Sulfide mineralization and dolomite brecciation has been shown to be closely related to syn-sedimentary faulting in the Irish Midlands; however, facies changes

and thickness variations are not as prevalent as in the strata of northwest Ireland (Gregg *et al*., 2001; Nagy *et al*., 2005).

T_h values of fluid inclusions from sphalerite and associated dolomite at Abbeytown and TQ/TWC indicate a lower temperature of ore formation in northwest Ireland than in the Irish Midlands (Wilkinson, 2003; Johnson *et al*., in press). This variation can be explained either by fluids circulating to a lesser depth in northwest Ireland, or a lower regional geothermal gradient at the time of mineralization. An abnormally high geothermal gradient has been suggested in the Irish Midlands. Jones (1992) suggested a geothermal gradient of 40 °C/km using conodont CAI values and Sevastopulo and Redmond (1999) suggested a geothermal gradient of 45-50 °C/km based on sediment thickness. Strogen *et al*. (1990) measured a geothermal gradient of 75 °C/km at the Navan deposit (Fig. 1). Host dolomite $\delta^{18}O$ values at Abbeytown and TWC/TQ are lower than values reported in planar and nonplanar dolomitized Waulsortian Limestone in the Irish Midlands (Gregg *et al*., 2001; Wright *et al.,* 2003). The values in northwest Ireland do however resemble the values of neomorphosed replacement dolomite recorded by Wright *et al*. (2003). Host dolomite $\delta^{13}C$ values in northwest Ireland are similar to those reported in the Irish Midlands. It is likely that a similar fluid-mixing system is responsible for ore formation in northwest Ireland as has been shown in the Irish Midlands and deposits of the northwest Ireland region may be considered a lower temperature (110-160 °C) variation of an Irish-type Pb-Zn deposit.

Comparison to mineralization in the Maritimes Basin, Nova Scotia

Mississippian carbonate-hosted Pb-Zn mineralization in the Maritimes Basin of Nova Scotia, Canada has been identified as epigenetic deposits similar to Mississippi Valley-type (MVT) and Irish-type deposits. During the late Paleozoic the area of the Maritimes Basin was in close proximity to the Sligo area (Scotese, 2002) and may have undergone similar geologic processes. Fallara and Savard (1998) noted that dolomitization and mineralization in Nova Scotia appears to be closely related to faults, with lead and zinc concentrations decreasing away from these faults. Sangster *et al*. (1998) determined that metal ions were obtained by fluids circulating through these faults from underlying siliciclastics, although a contribution from basement rocks was likely present. Fluid inclusion data presented by Kontak (1998) and carbon and oxygen stable isotope data from Savard and Kontak (1998) both indicate the presence of multiple fluids in the mineralized area. These studies concluded that ore formation was a result of mixing of a deeply sourced, high temperature, metal-rich brine with a shallower, evaporitic fluid possibly related to thick evaporite deposits of the Asbian-age Windsor Group (Kontak, 1998; Savard and Kontak, 1998). A third, low salinity fluid was observed by Kontak (1998) to postdate ore formation.

The genesis of the Maritimes Basin deposits is similar to that for mineralization in northwest Ireland with regard to their dependence on structural features and the presence of multiple mineralizing fluids. However, homogenization temperatures from ore-stage minerals in the Gays River Deposit in Maritimes Basin extend much higher (120-240 °C) (Kontak, 1998) than those measured from Abbeytown. This temperature range is similar to typical Irish-type sulfide deposits in the Rathdowney Trend (150-280 °C from

Johnston, 1999) and may be a result of deeper circulation or a higher geothermal gradient than that in northwest Ireland. Salinities calculated by Kontak (1998) also are higher than those measured in northwest Ireland (20-30 wt. % NaCl) but more closely resemble inclusions from the Irish Midlands (Johnson *et al*., in press). This may be a result of a higher degree of evaporation of seawater in the Maritimes Basin.

CHAPTER VI

CONCLUSIONS

Optical and cathodoluminescence petrography, fluid inclusion microthermometry and stable isotope geochemistry from epigenetic carbonate cements and sulfide mineralization from four sampled localities in northwest Ireland allows for a regional evaluation of diagenetic processes and fluid flow history.

1. Petrography indicates that host Ballyshannon and Dartry Limestones are sedimentologically similar on both the east and west sides of the Ox Mountains Inlier. Carbon and oxygen isotope data indicate that host limestones at the four sampled localities are equivalent geochemically. This is consistent with recent lithofacies distribution mapping and faunal correlations conducted by Somerville *et al*. (in prep.) that suggest northwest Ireland was a single carbonate platform in the Upper Viséan. Petrography and stable isotope data from host dolomite from Abbeytown Mine and quarry, Twigspark and Trotter's Quarries, and O'Donnell's Rock indicate that diagenetic processes during host rock dolomitization were not consistent regionally.
2. The more notable mineral paragenetic differences are between localities to the west and to the east of the Ox Mountains Inlier. This may indicate that late stage mineralization formed after significant uplift of the Inlier had occurred.

Initial movement of faults associated with the uplift has been dated to be Arundian to Asbian (Hitzman, 1986; Somerville *et al*., in prep.). This provides the earliest possible timing of mineralization in northwest Ireland.

3. Each of the four areas appears to have different fluid histories as indicated by cathodoluminescence, fluid inclusion and stable isotope data. Fluid inclusion data from Abbeytown and Twigspark/Trotter's Quarry suggest the involvement (mixing) of three geochemically distinct fluids. The interaction of two of these fluids, a lower-temperature, higher-salinity fluid and a higher-temperature, moderate-salinity fluid was vital to ore formation at Abbeytown and sulfide mineralization at Twigspark. At O'Donnell's Rock and Tate's Quarry no sulfide mineralization was present and one or both of these fluids was missing at each locality.
4. No regional fluid system, as has been proposed in the Irish Midlands, is indicated in northwest Ireland. Significant uplift of Proterozoic metamorphic rocks is indicated to have predated mineralization in the region. The absence of a regional cathodoluminescence microstratigraphy in epigenetic carbonate cements, differing paragenetic sequences, and the observation of geochemically diverse fluids at each study area suggests that each locality was isolated geologically at the time of sulfide mineralization.

REFERENCES

BANKS, D.A., Boyce, A.J. and Samson, I.M., 2002, Constraints on the origins of fluids forming Irish Zn-Pb-Ba deposits: evidence from the composition of fluid inclusions: *Economic Geology*, **97**, 471-480.

BODNAR, R.J., 1992, Revised equation and table for freezing point depressions of H_2O-salt fluid inclusions: *Program and abstracts: fourth biennial Pan-American Conference on Research on Fluid Inclusions*, **4**, 15.

CHARLESWORTH, J. K., 1953, *The Geology of Ireland*: Edinburgh, Oliver & Boyd Ltd., 276 pp.

CHEW, D.M., Daly, J.S., Page, L.M. and Kennedy, M.J., 2003, Grampian orogenesis and the development of blueschist-facies metamorphism in western Ireland: *Journal of the Geological Society, London*, **160**, 911-924.

CÓZAR, P., Somerville, I.D., Aretz, M. and Herbig, H.G., 2005, Biostratigraphic dating of Upper Visean limestones (NW Ireland) using foraminifera, calcareous algae and rugose corals: *Irish Journal of Earth Sciences*, **23**, 1-23.

CÓZAR, P., Somerville, I.D., Mitchell, W.I. and Medina-Varea, P., 2006, Correlation of Mississippian (Upper Viséan) foraminiferan, conodont, miospore and ammonoid zonal schemes and correlation with the Asbian-Brigantian boundary in northwest Ireland: *Geological Journal*, **41**, 221-241.

FALLARA, F. and Savard, M.M., 1998, A structural, petrographic, and geochemical study of the Jubilee Zn-Pb deposit, Nova Scotia, Canada, and a new metallogenic model: *Economic Geology*, **93**, 757-778.

GEORGE, T.N., Johnson, G.A.L., Mitchell, M., Prentice, J.E., Ramsbottom, W.H.C., Sevastopulo, G.D. and Wilson, R.B., 1976, A Correlation of Dinantian Rocks in the British Isles: *Geological Society, London*, Report No. 7, 87 pp.

GOLDSTEIN, R.H. and Reynolds, T.J., 1994, *Systematics of fluid inclusions in diagenetic minerals*: Tulsa, OK, Society for Sedimentary Geology, 199 p.

GREGG, J.M., Shelton, K.L., Johnson, A.W., Somerville, I.D. and Wright, W.R., 2001, Dolomitization of the Waulsortian Limestone (Lower Carboniferous) in the Irish Midlands: *Sedimentology*, **48**, 745-766.

HITZMAN, M.W., 1986, Geology of the Abbeytown mine, Co. Sligo, Ireland, *in* Andrew, C.J., Crowe, R.W.A., Finlay, S., Pennell, W.M. and Pyne, J.F., eds., *Geology and Genesis of Mineral Deposits in Ireland*: Dublin, Ireland, Irish Association for Economic Geology, 341-353.

HITZMAN, M.W., Allan, J.R. and Beaty, D.W., 1998, Regional dolomitization of the Waulsortian limestone in southeastern Ireland: Evidence of large-scale fluid flow driven by the Hercynian orogeny: *Geology*, **26**, 547-550.

HITZMAN, M.W. and Beaty, D.W., 1996, The Irish Zn-Pb-(Ba) orefield: *Society of Economic Geologists Special Publication*, **4**, 112-143.

JOHNSON, A.W., Shelton, K.L., Gregg, J.M., Somerville, I.D. and Wright, W.R., In review, Regional studies of the dolomites and their included fluids: Recognizing multiple chemically distinct fluids during the complex diagenetic history of the Irish Zn-Pb ore field: *Mineralogy and Petrology*.

JOHNSTON, J.D., 1995a, Major northwest-directed Caledonian thrusting and folding in Precambrian rocks, northwest Mayo, Ireland: *Geological Mag.*, **132**, 91-113.

JOHNSTON, J.D., 1995b, Variscan deformation in Ireland, *in* Anderson, K., Ashton, J., Earls, G., Hitzman, M., and Tear, S., eds., Irish Carbonate-Hosted Zn-Pb Deposits, *Soc. Econ. Geol. Guidebook Series*, **21**, 111-113.

JOHNSTON, J.D. and Phillips, W.E.A., 1995, Terrane amalgamation in the Clew Bay region, west of Ireland: *Geological Mag.*, **132**, 485-501.

JOHNSTON, J.D., 1999, Regional fluid flow and the genesis of Irish Carboniferous base metal deposits: *Mineralium Deposita*, **34**, 571-598.

JONES, G.Ll., 1992, Irish Carboniferous conodonts record maturation levels and the influence of tectonism, igneous activity and mineralization: *Terra Nova*, **4**, 238-244.

KELLY, J., 2007, A history of Zn-Pb-Ag mining at Abbeytown: *Journal of the Mining Heritage Trust of Ireland*, **7**, 17-26.

KONTAK, D.J., 1998, A study of fluid inclusions in sulfide and nonsulfide mineral phases from a carbonate-hosted Zn-Pb deposit, Gays River, Nova Scotia, Canada: *Economic Geology*, **93**, 793-817.

MACDERMOT, C.V., Long, C.B. and Harney, S.J., 1996, *Geology of Sligo-Leitrim. A geological description of Sligo, Leitrim and adjoining parts of Cavan, Fermanagh, Mayo and Roscommon, to accompany bedrock geology 1:100,000 scale map series, Sheet 7, Sligo-Leitrim*: Geological Survery of Ireland, Dublin, 100 pp.

MENNING, M., Alekseev, A.S., Chuvashov, B.I., Davydov, V.I., Devuyst, F.X., Forke, H.C., Grunt, T.A., Hance, L., Heckel, P.H., Izokh, N.G., Jin, Y-G., Jones, P.J., Kotlyar, G.V., Kozur, H.W., Nemyrovska, T.I., Schneider, J.W., Wang, X-D., Weddige, K., Weyer, D., and Work, D.M., 2006, Global time scale and regional stratigraphic reference scales of Central and West Europe, East Europe, Tethys, South China, and North America as used in the Devonian-Carboniferous-Permian Correlation Chart 2003 (DCP 2003): *Palaeogeography, Palaeoclimatology, Palaeoecology*, **240**, 318-372.

MITCHELL, W.I., 1992, The origin of Upper Palaeozoic sedimentary basins in Northern Ireland and relationships with the Canadian Maritime provinces, *in* Parnell, J., ed., *Basins on the Atlantic Seaboard: Petroleum Geology, Sedimentology and Basin Evolution*: Geol. Soc. Spec. Pub., **62**, 191-202.

MOLLOY, M.A. and Sanders, I.S., 1983, The NE Ox Mountains Inlier: Coolaney Area, *in* Archer, J. B. and Ryan P. D., eds., Geological Guide to the Caledonides of western Ireland: *Geological Survey of Ireland Guide Series*, **4**, 52-55.

NAGY, Z.R., Gregg, J.M., Shelton, K.L., Becker, S.P., Somerville, I.D., and Johnson, A.W., 2004, Early dolomitization and fluid migration through the Lower Carboniferous carbonate platform in the SE Irish Midlands: implications for reservoir attributes: *Geological Society, London, Spec. Pub.*, **235**, 367-392.

NAGY, Z.R., Somerville, I.D., Gregg, J.M., Becker, S.P., Shelton, K.L. and Sleeman, A.G., 2005, Sedimentation in an actively tilting half-graben: sedimentology and stratigraphy of Late Tournasian-Visean (Mississippian, Lower Carboniferous) carbonate rocks in south County Wexford, Ireland: *Sedimentology*, **52**, 489-512.

OSWALD, D.H., 1955, The Carboniferous rocks between the Ox Mountains and Donegal Bay: *Quarterly Journal of the Geological Society, London*, **111**, 167-186.

PHILCOX, M.E., Baily, H., Clayton, G., and Sevastopulo, G.D., 1992, Evolution of the Carboniferous Lough Allen Basin, Northwest Ireland: *Geological Society, London, Spec. Pub.*, **62**, 203-215.

POPP, B.N., Anderson, T.F. and Sandberg, P.A., 1986, Brachiopods as indicators of original isotopic compositions in some Paleozoic limestones: *Geological Society of America Bulletin*, **97**, 1262-1269.

PRICE, C. and Max, M.D., 1988, Surface and deep structural control of the NW Carboniferous Basin of Ireland: seismic perspectives of aeromagnetic and surface geological interpretation: *Journal of Petroleum Geology*, **11**, 365-388.

RAYNER, D.H., 1981, *The Stratigraphy of the British Isles*. Cambridge: Cambridge University Press, 460 pp.

ROSENBAUM, J. and Sheppard S.M.F., 1986, An isotopic study of siderites, dolomites and ankerites at high temperatures: *Geochimica et Cosmochimica Acta*, **50**, 1147-1150.

RUSSELL, M.J., 1978, Downward-excavating hydrothermal cells and Irish-type ore deposits: importance of an underlying thick Caledonian prism: *Trans. Insn. Min. Metall.*, **87**, 168-171.

RUSSELL, M.J., 1986, Extension and convection: a genetic model for the Irish Carboniferous base-metal and barite deposits, *in* Andrew, C.J., Crowe, R.W.A., Finlay, S., Pennell, W.M. and Pyne, J.F., eds., *Geology and Genesis of Mineral Deposits in Ireland*: Dublin, Ireland, Irish Association for Economic Geology, 545-554.

SANGSTER, D.F., Savard, M.M. and Kontak, D.J., 1998, Sub-basin-specific Pb and Sr sources in Zn-Pb deposits of the Lower Windsor Group, Nova Scotia, Canada: *Economic Geology*, **93**, 911-919.

SAVARD, M.M. and Kontak, D.J., 1998, $\delta^{13}C$, $\delta^{18}O$, $^{87}Sr/^{86}Sr$ covariations in ore-stage calcites at and around the Gays River Zn-Pb deposit (Nova Scotia, Canada); evidence for fluid mixing: *Economic Geology*, **93**, 818-833.

SCOTESE, C.R., 2002, Paleomap project, http://www.scotese.com/earth.htm.

SEVASTOPULO, G.D. and Redmond, P., 1999, Age of mineralization of carbonate-hosted, base metal deposits in the Rathdowney Trend, Ireland, *in* McCaffrey, K.J.W., Lonergan, L. and Wilkinson, J.J., eds., Fractures, Fluid Flow and Mineralization, *Geological Society, London, Spec. Pub.*, **151**, 303-311.

SIBLEY, D.F. and Gregg, J.M., 1987, Classification of dolomite rock textures: *Journal of Sedimentary Petrology*, **57**, 967-975.

SOMERVILLE, I.D., Cozar, P., Aretz, M., Herbig, H., Mitchell, W.I., and Medina-Varea, P., In review, Carbonate facies and biostromal distribution in the tectonically controlled platform in northwest Ireland during the late Viséan (Mississippian).

STROGEN, P., Jones, G.Ll. and Somerville, I.D., 1990, Stratigraphy and sedimentology of Lower Carboniferous (Dinantian) boreholes from west Co. Meath, Ireland: *Geological Journal*, **25**, 103-137.

THOMAS, C.W., Graham, C.M., Ellam, R.M. and Fallick, A.E., 2004, $^{87}Sr/^{86}Sr$ chemostratigraphy of Neoproterozoic Dalradian limestones of Scotland and Ireland: constraints on depositional ages and time scales: *Journal of the Geological Society, London*, **161**, 229-242.

WEST, M., Brandon, A. and Smith, M., 1968, A tidal flat evaporitic facies in the Visean of Ireland: *Journal of Sedimentary Petrology*, **38**, 1079-1093.

WILKINSON, J.J. and Earls, G., 2000, A high-temperature hydrothermal origin for black dolomite matrix breccias in the Irish Zn-Pb orefield: *Mineral. Mag*., **64**, 1017-1036.

WILKINSON, J.J., 2003, On diagenesis, dolomitisation and mineralization in the Irish Zn-Pb orefield: *Mineral Deposita*, **38**, 968-983.

WILKINSON, J.J., Everett, C.E., Boyce, A.J., Gleeson, S.A., and Rye, D.M., 2005, Intracratonic crustal seawater circulation and the genesis of subseafloor zinc-lead mineralization in the Irish orefield: *Geology*, **33**, 805-808.

WORONICK, R.E. and Land, L.S., 1985, Late burial diagenesis, Lower Cretaceous Pearsall and Lower Glen Rose Formations, south Texas, *in* Schneidermann, N., and Harris P.M., eds., Carbonate Cements: *SEPM Special Publication*, **36**, 265-275.

WRIGHT, W.R., 2001, Dolomitization, Fluid-Flow and Mineralization of the Lower Carboniferous Rocks of the Irish Midlands and Dublin Basin Regions [Ph.D. dissertation]: University College Dublin.

WRIGHT, W.R., Somerville, I.D., Gregg, J.M., Shelton, K.L. and Johnson, A.W., 2001, Application of regional dolomite cement CL (Cathodoluminescence) microstratigraphy to the genesis of Zn-Pb mineralization in Lower Carboniferous rocks, Ireland: Similarities to the Southeast Missouri Pb-Zn District?, *in* Hagni, R.D., ed., Studies on Ore Deposits, Mineral Economics and Applied Mineralogy: With Emphasis on Mississippi Valley-type Base Metal and Carbonatite-related Ore Deposits, University of Missouri-Rolla Press, Rolla, MO, 1-17.

WRIGHT, W.R., Somerville, I.D., Gregg, J.M., Johnson, A.W. and Shelton, K.L., 2003, Dolomitization and neomorphism of Irish Lower Carboniferous (Early Mississippian) limestones: Evidence from petrographic and isotopic studies, *in* Ahr, W.M., Harris, P.M., Morgan, W.A. and Somerville, I.D., eds., Permo-Carboniferous Platforms and Reefs, *SEPM/AAPG Spec. Pub*., **78**, 395-408.

WRIGHT, W.R., Somerville, I.D., Gregg, J.M., Shelton, K.L. and Johnson, A.W., 2004, The petrogenesis of dolomite, regional patterns of dolomitization and fluid flow in the Lower Carboniferous of the Irish Midlands and Dublin Basin, *in* Braithwaite,

C.J.R., Rizzi, G. and Darke, G., eds., The Geometry and Petrogenesis of Dolomite Hydrocarbon Reservoirs, *Geol. Soc. Spec. Publ.,* **235**, 75-97.

APPENDICES

Appendix 1 – Catalog of collected samples

Catalog of sample collected from field examinations in NW Ireland. Sample location coordinates were measured at the time of collection by GPS. Coordinates are displayed in the Irish Grid coordinate system. Samples collected from Abbeytown western ore body are indicated.

Location	Sample Name	Location Coordinates	Field Description
Abbeytown	AT-1	65982, 29590	cross-bedded dolomitized grainstone
Abbeytown	AT-2		vuggy cemented dolomite just below cross-bedded grainstone
Abbeytown	AT-3		biomicritic limestone lower in the section
Abbeytown	AT-4		mineralized sample from cross-bedded dolomitized grainstone
Abbeytown	AT-5		large calcite crystal from mineralized vug
Abbeytown	AT-6	65939, 29544	dolomite with dolomite filled veins SW of AT-1, roughly equivalent bed but not cross-bedded
Abbeytown	AT-7	65719, 29537	cross-bedded dolomitized grainstone pyrite mineralization
Abbeytown	AT-8		overlying dolomitized micrite
Abbeytown	AT-9		large calcite from vug in same rock as AT-8
Abbeytown	AT-10		dolomitized brachiopod grainstone
Abbeytown (west)	AT-11	65708, 29486	undolomitized cross-bedded grainstone
Abbeytown (west)	AT-12		mineralized micrite from higher in section
Abbeytown (west)	AT-13		micrite with cross-veined calcite
Abbeytown	AM-1		sphalerite mineralization from Index Bed
Abbeytown	AM-2		cross-bedded dolomitized grainstone
Abbeytown	AM-3		galena, sphalerite, late calcite mineralization
Abbeytown	AM-4		host dolomite with calcite vein
Abbeytown	AM-5		high grade sphalerite mineralization calcite vein from lowest mine level
Abbeytown	AM-6		below the Index Bed, just above the flooded area
Abbeytown	AM-7		brecciated high grade mineralization with multiple generations of carbonate
Abbeytown	AM-8	65723, 29529	galena bearing, collected at surface near mine entrance
Abbeytown (west)	AM-9	65747, 29617	edge of western ore body

Abbeytown (west)	AM-10		large grained saddle dolomite cement
Abbeytown (west)	AM-11	65946, 29608	large saddle and small rhomb dolomite cements
Abbeytown (west)	AM-12		galena with calcite
Abbeytown (west)	AM-13		pyrite and calcite halo above Index Bed
Trotter's Quarry	TQ-1	85208, 41321	possible dolomite-limestone transition in quarry wall
Trotter's Quarry	TQ-2	85219, 41360	near mud mound structure, limestone-dolomite transition with cement filled vugs
Trotter's Quarry	TQ-3		dolomite with cement filled vugs
Trotter's Quarry	TQ-4		dolomite-limestone transition
Trotter's Quarry	TQ-5		limestone from mound flanking beds
Trotter's Quarry	TQ-6		mound core, limestone-dolomite transition
Trotter's Quarry	TQ-7		mound core with calcite vein
Trotter's Quarry	TR-1	85054, 41714	vuggy limestone just below shale contact
Trotter's Quarry	TR-2		mudmound with shale drapping beds, collected from contact
Trotter's Quarry	TR-3		mudmound with shale drapping beds, collected from float
Trotter's Quarry	TR-4	85039, 41640	possibly dolomitized mound core with stromatactis
Trotter's Quarry	TR-5		from eastern mud mound core
Trotter's Quarry	TR-6	85130, 41526	undolomitized mound core, stromatactis structures
Twigspark Quarry	TW-1	85575, 40494	pyrite and calcite mineralization
Twigspark Quarry	TW-2		galena mineralization
Twigspark Quarry	TW-3		dolomite veining
Twigspark Quarry	TW-4		chalcopyrite, galena, calcite, pyrite mineralization
Twigspark Core (TP96-3)	TWC-1	88 m. (depth)	calcite veining
Twigspark Core (TP96-3)	TWC-2	147 m.	dolomite with dolomite vein
Twigspark Core (TP96-3)	TWC-3	155 m.	dolomite with dolomite veins and calcite vugs
Twigspark Core (TP96-3)	TWC-4	191 m.	calcite veins in limestone
Twigspark Core (TP96-3)	TWC-5	268 m.	vuggy saddle dolomite
Twigspark Core (TP96-3)	TWC-6	292 m.	coarse grained dolomite grainstone
Twigspark Core (TP96-3)	TWC-7	319 m.	vuggy saddle dolomite
Twigspark Core (TP96-3)	TWC-8	356 m.	calcite with associated dolomite
Twigspark Core (TP96-3)	TWC-9	410 m.	basement schist with calcite veins
Twigspark Core (TP95-1)	TWC-10	229 m.	uppermost occurance of dolomite in core #2
Twigspark Core (TP96-1)	TWC-11	145 m.	calcite with pyrite

O'Donnell's Rock	OR-1	87973, 35194	dolomitized crinoidal limestone
O'Donnell's Rock	OR-2		partially dolomitized with calcite vein (slightly lower in the section)
O'Donnell's Rock	OD-1	87959, 35184	large quartz filled vug
O'Donnell's Rock	OD-2	88170, 35434	bedded limestone collected near the top
O'Donnell's Rock	OD-3	88167, 34762	dolomitized with calcite and dolomite vug
O'Donnell's Rock	OD-4		calcite vein with ferroan dolomite limestone with calcite and fluorite
Tate's Quarry	TAQ-1	91287, 39167	filled vug
Tate's Quarry	TA-1	91250, 39250	calcite filled vug
Tate's Quarry	TA-2	91264, 39138	calcite vug, quartz lined?
Tate's Quarry	TA-3		fossiliferous limestone
Tate's Quarry	TA-4		large calcite vug
Streedagh Point	SP-1	62892, 50657	N-S trending calcite veins in the Glencar Ls
Aghagrania River	AR-1	99593, 12052	top of Dartry Ls
	AR-2		base of Meenymore Fm
	AR-3		~ 3m. higher in the section (partly dolomitized?) with vertical veins
	AR-4		~ 2m. above AR-3, brecciated limestone with vertical veins
	AR-5		just above the brecciated unit
	AR-6		~ 6m. above AR-5, dolomitized micrite
	AR-7	99694, 12050	dolomitized micrite
	AR-8		just overlying AR-7, laminated limestone (water layed?)
	AR-9	99694, 12061	vuggy dolomite with quartz cement filling vugs, possible vein calcite & dolomite
	AR-10		vuggy dolomitized micrite with vugs filled by silica
	AR-11		laminated micrite
	AR-12		dolomitized breccia
	AR-13		~ 5m. higher in the section, dolomitized micrite with vertical veins
	AR-14		same as AR-13
	AR-15	99771, 12099	granular dolomite
	AR-16	99816, 12198	thin laminated partly dolomitized micritic limestone
	AR-17		3 m above AR-16, laminated dolomite
	AR-18		~ 7m above AR-17, laminated micrite at base, dolomitized at the top
	AR-19		laminated micrite, coarse at base
	AR-20		overlying breccia

	AR-21		~ 6m higher in section, lots of chert nodules, partly dolomitized laminated micrite
Kerrigan Quarry	KQ-1	86299, 30591	multiple calcite veins, possibly fault offsetting present
Kerrigan Quarry	KQ-2	86425, 30478	dolomite vugs from mud mound core
Kerrigan Quarry	KQ-3		pyrite mineralization with calcite vug in limestone

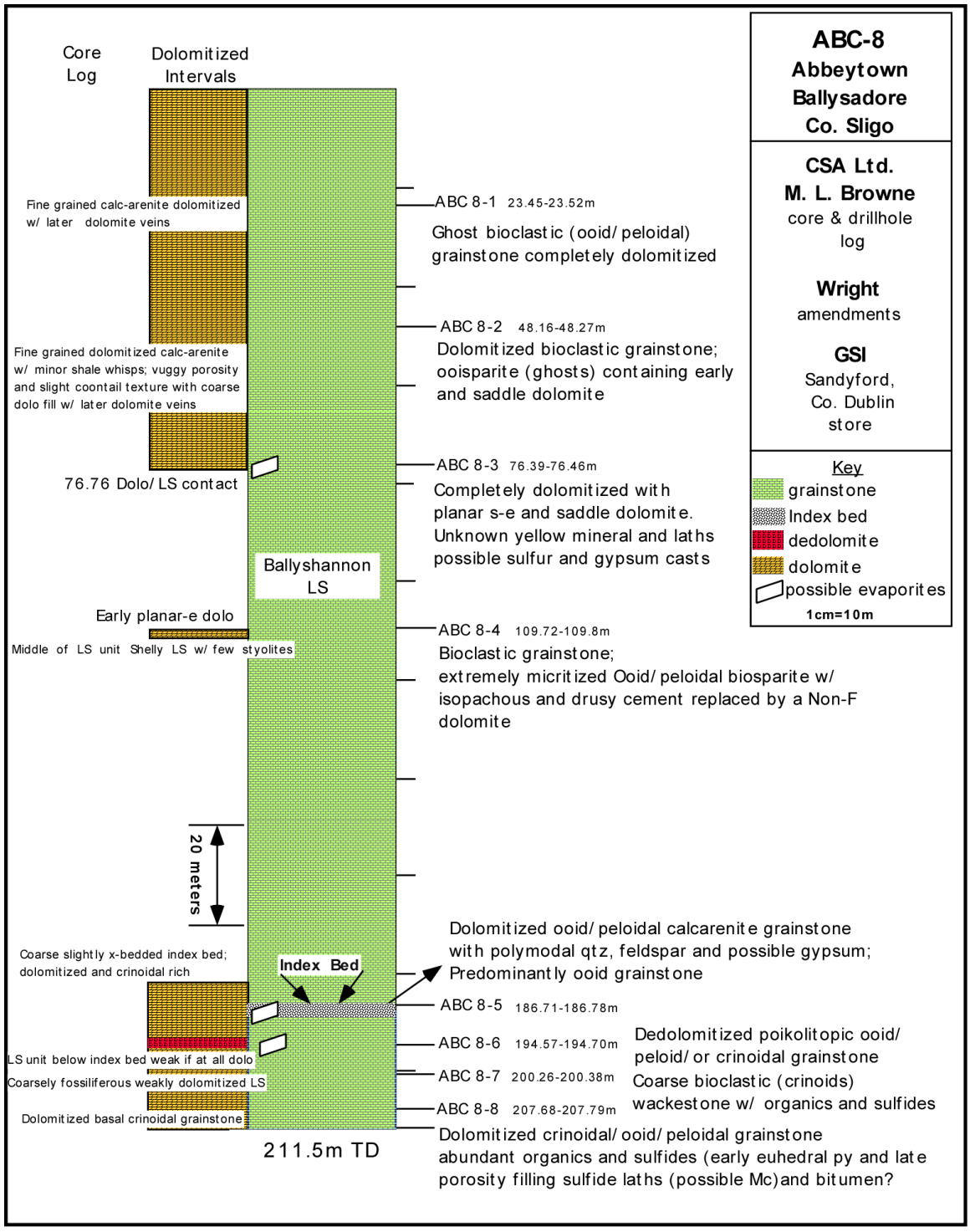

Log and sample descriptions of core ABC-8 from the Abbeytown Mine area; compiled by Wright (2001).

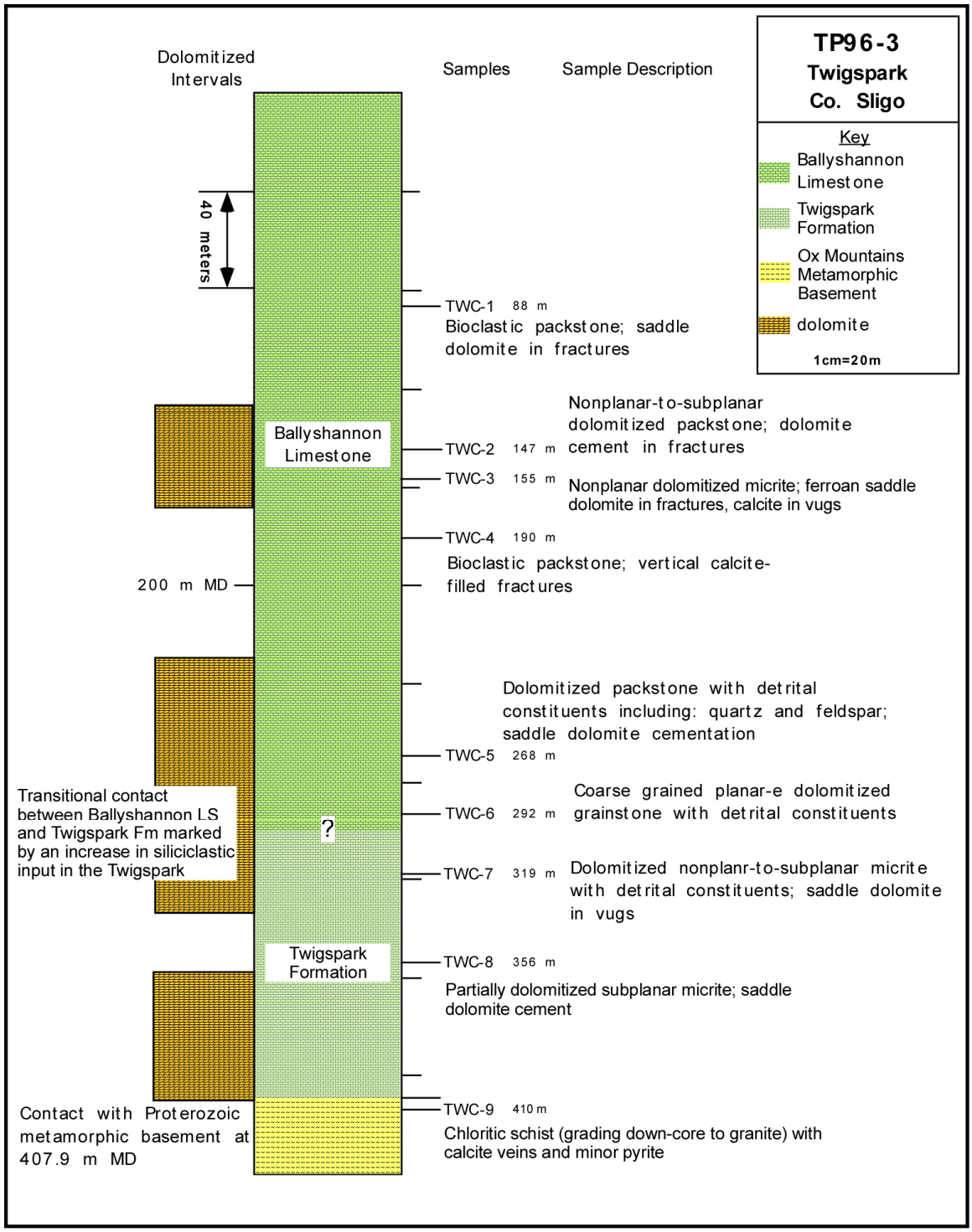

Log and sample descriptions of core TP96-3 from near Twigspark Quarry.

Appendix 3 – Fluid inclusion data

Homogenization temperature (T_h), temperature of first ice melt (T_{fm}) and final ice melting temperatures (T_m) of fluid inclusions in epigenetic cements from NW Ireland. Weight percent NaCl is converted from T_m values using equations from Bodnar (1992).

Sample	Mineral	T_h	T_{fm}	T_m	wt.%equiv. NaCl (Tm)
AT-2	calcite	143	-29.7	-2.6	4.34
AT-2	calcite	140	-28.1	-4.0	6.45
AT-2	calcite	145	-25.6	-2.5	4.18
AT-2	calcite	153	-33.1	-6.4	9.73
AT-2	calcite	155	-34.6	-7.2	10.73
AT-2	calcite	146	-31.0	-6.6	9.98
AT-2	calcite	135	-24.8	-4.4	7.02
AT-2	calcite	147	-24.5	-7.3	10.86
AT-2	calcite	139	-39.0	-5.6	8.68
AT-2	calcite	126	-40.5	-7.3	10.86
AT-2	calcite	145	-37.1	-7.4	10.98
AT-2	calcite	144	-38.8	-9.2	13.07
AT-2	calcite	138	-41.3	-10.1	14.04
AT-2	calcite	153	-42.0	-4.9	7.73
AT-2	calcite	143	-39.1	-9.7	13.62
AT-2	calcite	153	-32.5	-3.5	5.71
AT-2	calcite	144	-31.6	-8.0	11.70
AT-2	calcite	140	-29.0	-5.9	9.08
AT-2	calcite	134	-24.2	-5.8	8.95
AT-2	sphalerite	109	-37.3	-12.6	16.53
AT-2	sphalerite	158	-35.3	-7.7	11.34
AT-4	calcite	142	-38.4	-16.1	19.53
AT-4	calcite	140	-32.0	-16.0	19.45
AT-4	calcite	143	-28.0	-11.2	15.17
AT-4	calcite	98	-40.6	-15.3	18.88
AT-4	calcite	122	-35.8	-10.7	14.67
AT-4	calcite	118	-34.4	-8.4	12.16
AT-4	calcite	121	-32.9	-12.0	15.96
AT-4	calcite	163	-23.2	-7.4	10.98
AT-4	calcite	171	-27.4	-7.4	10.98
AT-4	calcite	159	-27.2	-7.6	11.22
AT-4	calcite	165	-23.8	-7.2	10.73
AT-4	calcite	121	-36.2	-10.0	13.94
AT-4	calcite	125	-42.3	-10.3	14.25

Sample	Mineral	T_h	T_{fm}	T_m	wt.% equiv. NaCl (Tm)
AT-4	calcite	187	-40.8	-6.8	10.24
AT-4	calcite	108	-22.3	-12.7	16.62
AT-4	calcite	130	-26.2	-7.4	10.98
AT-4	dolomite	128	-39.5	-4.9	7.73
AT-4	dolomite	134	-37.8	-6.6	9.98
AT-4	dolomite	140	-41.2	-5.8	8.95
AT-4	dolomite	137	-42.6	-5.6	8.68
AT-4	dolomite	136	-41.9	-11.2	15.17
AT-4	dolomite	197	-34.2	-9.1	12.96
AT-4	dolomite	184	-39.6	-8.3	12.05
AT-4	dolomite	179	-38.4	-9.0	12.85
AT-4	dolomite	168	-35.0	-7.0	10.49
AT-4	dolomite	171	-29.4	-8.3	12.05
AT-4	dolomite	129	-45.0	-4.1	6.59
AT-4	dolomite	108	-45.2	-3.3	5.41
AT-4	dolomite	113	-39.2	-6.5	9.86
AT-4	dolomite	124	-40.9	-4.0	6.45
AT-4	dolomite	120	-44.3	-6.0	9.21
AT-4	dolomite	192	-44.4	-6.7	10.11
AT-4	dolomite	185	-30.8	-6.9	10.36
AT-4	dolomite	192	-32.4	-8.0	11.70
AT-9	calcite	178	-22.4	-6.6	9.98
AT-9	calcite	175	-23.3	-6.8	10.24
AT-9	calcite	187	-25.8	-8.5	12.28
AT-9	calcite	175	-22.6	-7.1	10.61
AT-9	calcite	179	-30.6	-9.3	13.18
AT-9	calcite	174	-28.4	-6.1	9.34
AT-9	calcite	208	-25.2	-4.8	7.59
AT-9	calcite	141	-26.8	-7.4	10.98
AT-9	calcite	168	-28.1	-5.7	8.81
AT-9	calcite	222	-22.5	-4.0	6.45
AT-9	calcite	190	-29.7	-6.8	10.24
AT-9	calcite	179	-26.7	-7.1	10.61
AT-9	calcite	168	-26.1	-7.5	11.10
AT-9	calcite	155	-25.9	-8.0	11.70
AT-9	calcite	175	-25.0	-7.8	11.46
AT-9	calcite	136	-26.0	-6.5	9.86
AT-9	dolomite	175	-19.1	-7.9	11.58
AT-9	dolomite	178	-27.8	-9.4	13.29
AT-9	dolomite	185	N/A	N/A	N/A
AT-9	dolomite	188	N/A	N/A	N/A

Sample	Mineral	T_h	T_{fm}	T_m	wt.% equiv. NaCl (Tm)
AT-9	dolomite	168	-27.9	-9.1	12.96
AT-9	dolomite	171	N/A	N/A	N/A
AT-9	dolomite	173	-24.6	-7.9	11.58
AT-9	dolomite	176	-25.8	-7.0	10.49
AT-9	dolomite	173	-25.1	-6.0	9.21
AT-9	dolomite	146	-31.0	-4.8	7.59
AT-9	dolomite	143	-32.1	-5.0	7.86
AT-9	dolomite	135	-27.4	-4.7	7.45
AT-9	dolomite	138	-30.0	-8.0	11.70
AT-9	dolomite	207	-29.5	-7.0	10.49
AT-9	dolomite	115	-24.0	-5.3	8.28
AT-9	dolomite	143	-21.9	-4.0	6.45
AT-9	dolomite	157	-23.4	-7.5	11.10
AT-9	dolomite	160	-26.9	N/A	N/A
AT-9	dolomite	182	-29.2	-10.4	14.36
AT-9	dolomite	178	-23.0	-8.0	11.70
AT-9	dolomite	173	-27.6	-6.8	10.24
AM-5	sphalerite	119	-33.7	-11.2	15.17
AM-5	sphalerite	142	-36.8	-10.3	14.25
AM-5	sphalerite	132	-31.1	-9.0	12.85
AM-5	sphalerite	123	-36.5	-11.0	14.97
AM-5	sphalerite	146	-43.7	-9.8	13.72
AM-5	sphalerite	143	-37.7	-7.1	10.61
AM-5	sphalerite	125	-36.5	-10.8	14.77
AM-5	sphalerite	116	-35.4	-9.8	13.72
AM-5	sphalerite	118	-34.5	-9.4	13.29
AM-5	sphalerite	137	-33.2	-7.3	10.86
AM-5	sphalerite	134	-38.2	-7.8	11.46
AM-5	sphalerite	109	-37.3	-12.6	16.53
AM-5	sphalerite	158	-35.3	-7.7	11.34
AM-8	calcite	147	-28.0	-7.7	11.34
AM-8	calcite	152	-25.8	-5.1	8.00
AM-8	calcite	144	-24.2	-5.8	8.95
AM-8	calcite	146	-24.8	-7.3	10.86
AM-8	calcite	157	-27.4	-8.0	11.70
AM-8	calcite	178	-27.6	-9.1	12.96
AM-8	calcite	176	-28.3	-9.3	13.18
AM-8	calcite	168	-30.0	-9.0	12.85
AM-8	calcite	131	-23.4	-6.3	9.60
AM-8	calcite	124	-22.8	-4.0	6.45
AM-8	calcite	134	-22.3	-5.8	8.95

Sample	Mineral	T_h	T_{fm}	T_m	wt.% equiv. NaCl (Tm)
AM-8	calcite	127	-23.0	-5.0	7.86
AM-8	calcite	129	-22.5	-5.5	8.55
AM-8	calcite	130	-25.2	-3.2	5.26
AM-8	calcite	124	-23.6	-6.4	9.73
AM-8	calcite	122	-23.4	-6.0	9.21
AM-8	sphalerite	156	-27.9	N/A	N/A
AM-8	sphalerite	168	-31.5	-7.0	10.49
AM-8	sphalerite	135	-23.7	N/A	N/A
AM-8	sphalerite	119	-30.3	-10.9	14.87
AM-8	sphalerite	151	-29.7	-11.0	14.97
AM-8	sphalerite	154	-29.3	-11.3	15.27
AM-8	sphalerite	146	-29.2	-11.5	15.47
AM-8	sphalerite	120	-31.6	-11.3	15.27
AM-8	sphalerite	112	-29.1	-11.6	15.57
AM-8	sphalerite	114	-28.4	-8.4	12.16
AM-8	sphalerite	132	-24.3	-9.4	13.29
AM-8	sphalerite	124	-26.0	-10.3	14.25
AM-8	sphalerite	133	-37.2	-12.6	16.53
AM-8	sphalerite	110	-28.3	-11.7	15.67
AM-9	calcite	99	-24.8	-2.9	4.80
AM-9	calcite	98	-31.8	-3.7	6.01
AM-9	calcite	107	-31.1	-15.7	19.21
AM-9	calcite	92	-24.0	-12.3	16.24
AM-9	calcite	102	-28.8	-12.1	16.05
AM-9	calcite	115	-31.9	-12.7	16.62
AM-9	calcite	74	-27.6	-3.4	5.56
AM-9	calcite	111	-28.1	-5.6	8.68
AM-9	calcite	121	-35.1	-18.5	21.33
AM-9	calcite	113	-29.4	-5.8	8.95
AM-9	calcite	92	-30.6	-12.7	16.62
AM-9	calcite	87	-35.8	-12.4	16.34
AM-9	calcite	109	-29.5	-20.4	22.65
AM-9	calcite	111	-26.7	-14.2	17.96
AM-9	calcite	89	-32.8	-16.2	19.60
AM-9	calcite	71	-27.6	-3.2	5.26
AM-9	calcite	114	-36.5	-13.2	17.08
AM-9	calcite	95	-25.4	-2.6	4.34
AM-9	calcite	74	-26.6	-18.9	21.61
AM-9	calcite	70	-28.4	-15.9	19.37
AM-9	calcite	102	-25.0	-20.4	22.65
AM-9	calcite	83	-24.3	-5.0	7.86

Sample	Mineral	T_h	T_{fm}	T_m	wt.% equiv. NaCl (Tm)
AM-9	dolomite	142	-31.0	-6.0	9.21
AM-9	dolomite	117	-29.5	-3.8	6.16
AM-9	dolomite	116	-34.0	-4.9	7.73
AM-9	dolomite	117	-41.7	-4.5	7.17
AM-9	dolomite	116	-36.8	-5.5	8.55
AM-9	dolomite	136	-31.5	-4.4	7.02
AM-9	dolomite	105	-40.2	-2.7	4.49
AM-9	dolomite	134	-34.1	-5.7	8.81
AM-9	dolomite	124	-30.4	-4.3	6.88
AM-9	dolomite	140	-28.2	-9.7	13.62
AM-9	dolomite	144	-28.3	-5.5	8.55
AM-9	dolomite	121	-29.7	-5.1	8.00
AM-9	dolomite	126	-23.0	-4.0	6.45
AM-9	dolomite	120	-27.8	-5.3	8.28
AM-9	dolomite	168	-30.4	-6.8	10.24
AM-9	dolomite	133	-29.7	-5.9	9.08
AM-9	dolomite	117	-29.6	-3.2	5.26
AM-9	dolomite	130	-25.7	-5.8	8.95
AM-11	dolomite	165	-23.4	-4.7	7.45
AM-11	dolomite	159	-25.1	-4.6	7.31
AM-11	dolomite	161	-26.2	-3.5	5.71
AM-11	dolomite	147	-25.9	-4.1	6.59
AM-11	dolomite	153	-32.8	-4.7	7.45
AM-11	dolomite	161	-27.1	-6.6	9.98
AM-11	dolomite	138	-24.6	-7.1	10.61
AM-11	dolomite	173	-25.4	-7.0	10.49
AM-11	dolomite	145	-22.5	-4.2	6.74
AM-11	dolomite	142	-22.3	-4.5	7.17
AM-11	dolomite	158	-20.2	-6.1	9.34
AM-11	dolomite	135	-41.3	-8.3	12.05
AM-11	dolomite	140	-42.2	-11.0	14.97
AM-11	dolomite	138	-39.0	-7.9	11.58
AM-11	dolomite	150	-43.0	-10.8	14.77
AM-11	dolomite	156	-33.8	-6.6	9.98
AM-11	dolomite	150	-25.9	-6.2	9.47
AM-11	dolomite	147	-31.2	-4.5	7.17
AM-11	dolomite	158	-39.5	-10.0	13.94
AM-11	dolomite	153	-38.2	-9.2	13.07
AM-11	dolomite	157	-41.1	-8.1	11.81
AM-11	dolomite	147	-28.1	-4.8	7.59
AM-11	dolomite	127	-27.0	-5.9	9.08

Sample	Mineral	T_h	T_{fm}	T_m	wt.% equiv. NaCl (Tm)
AM-11	dolomite	128	-23.8	-4.0	6.45
AM-11	dolomite	124	-25.5	-9.6	13.51
TQ-2	dolomite	124	-41.8	-7.5	11.10
TQ-2	dolomite	120	-38.5	-6.6	9.98
TQ-2	dolomite	158	-26.4	-4.6	7.31
TQ-2	dolomite	124	-22.8	-5.6	8.68
TQ-2	dolomite	157	-21.3	-5.8	8.95
TQ-2	dolomite	198	-25.7	-8.1	11.81
TQ-2	dolomite	117	-31.2	-7.7	11.34
TQ-2	dolomite	121	-26.8	-6.3	9.60
TQ-2	dolomite	112	-30.1	-6.0	9.21
TQ-2	dolomite	137	-27.7	-3.9	6.30
TQ-2	dolomite	123	-31.4	-3.6	5.86
TQ-2	dolomite	131	-39.3	-5.0	7.86
TQ-2	dolomite	113	-32.4	-3.8	6.16
TQ-2	dolomite	159	-29.3	-6.8	10.24
TQ-2	dolomite	160	-31.0	-5.2	8.14
TQ-2	dolomite	163	-27.1	-7.5	11.10
TQ-2	dolomite	165	-31.5	-7.3	10.86
TQ-2	dolomite	135	-41.0	-7.5	11.10
TQ-2	dolomite	118	-29.8	-3.5	5.71
TQ-2	dolomite	131	-33.8	-7.8	11.46
TQ-2	dolomite	119	-36.2	-9.2	13.07
TQ-2	dolomite	146	-35.8	-5.0	7.86
TQ-2	dolomite	133	-31.9	-3.7	6.01
TQ-2	dolomite	95	-32.5	-6.4	9.73
TQ-2	dolomite	102	-33.8	-6.7	10.11
TR-1	calcite	99	-33.0	-3.9	6.30
TR-1	calcite	110	-27.9	-5.8	8.95
TR-1	calcite	114	-40.0	-8.0	11.70
TR-1	calcite	129	-26.7	-4.4	7.02
TR-1	calcite	133	-26.7	-4.7	7.45
TR-1	calcite	137	-22.7	-3.6	5.86
TR-1	calcite	111	-26.8	-1.0	1.74
TR-1	calcite	113	-33.5	-1.4	2.41
TR-1	calcite	107	-23.4	-1.3	2.24
TR-1	calcite	97	-30.8	-5.7	8.81
TR-1	calcite	139	-24.0	-10.2	14.15
TR-1	calcite	132	-24.6	-5.8	8.95
TR-1	calcite	127	-23.7	-5.6	8.68
TR-1	calcite	130	-24.0	-5.8	8.95

Sample	Mineral	T_h	T_{fm}	T_m	wt.% equiv. NaCl (Tm)
TR-1	calcite	109	-26.7	-1.2	2.07
TR-1	calcite	188	-44.2	-4.2	6.74
TR-1	calcite	108	-31.5	-0.8	1.40
TR-1	calcite	84	-23.2	-4.2	6.74
TR-1	calcite	88	-23.2	-4.3	6.88
TW-1	calcite	160	-35.1	-11.2	15.17
TW-1	calcite	208	-41.3	-8.1	11.81
TW-1	calcite	124	-42.8	-6.5	9.86
TWC-3	calcite	99	-55.6	-16.2	19.60
TWC-3	calcite	139	-41.2	-7.7	11.34
TWC-3	calcite	132	-42.2	-8.1	11.81
TWC-3	calcite	175	-35.1	-11.6	15.57
TWC-3	calcite	89	-27.5	-16.3	19.68
TWC-3	calcite	96	-25.5	-15.8	19.29
TWC-3	calcite	81	-23.1	-15.7	19.21
TWC-3	calcite	113	-37.0	-10.4	14.36
TWC-3	calcite	121	-35.0	-10.7	14.67
TWC-3	calcite	81	-27.8	-14.8	18.47
TWC-3	calcite	86	-23.4	-14.5	18.22
TWC-3	calcite	127	-42.2	-10.5	14.46
TWC-3	calcite	90	-28.1	-15.5	19.05
TWC-3	calcite	84	-33.1	-15.1	18.72
TWC-3	calcite	113	-28.0	-6.2	9.47
TWC-3	calcite	135	-32.1	-4.3	6.88
TWC-3	calcite	81	-39.7	-16.3	19.68
TWC-3	calcite	90	-28.8	-16.4	19.76
TWC-3	calcite	87	-28.9	-13.1	16.99
TWC-3	calcite	89	-39.0	-16.1	19.53
TWC-3	calcite	127	-26.9	-11.0	14.97
TWC-3	calcite	74	-34.6	-12.6	16.53
TWC-3	calcite	91	-28.7	-12.7	16.62
TWC-3	dolomite	136	-46.3	-7.9	11.58
TWC-3	dolomite	130	-31.2	-4.1	6.59
TWC-3	dolomite	140	-36.8	-4.8	7.59
TWC-3	dolomite	129	-42.0	-16.1	19.53
TWC-3	dolomite	166	-42.1	-16.3	19.68
TWC-3	dolomite	125	-37.1	-15.5	19.05
TWC-3	dolomite	123	-44.2	-13.5	17.34
TWC-3	dolomite	125	-36.2	-9.1	12.96
TWC-3	dolomite	118	-23.1	-16.0	19.45
TWC-3	dolomite	133	-33.3	-9.2	13.07

Sample	Mineral	T_h	T_{fm}	T_m	wt.% equiv. NaCl (Tm)
TWC-3	dolomite	106	-47.0	-15.0	18.63
TWC-3	dolomite	121	-30.5	-15.1	18.72
TWC-3	dolomite	134	-39.9	-12.3	16.24
TWC-3	dolomite	115	-26.9	-15.6	19.13
TWC-3	dolomite	121	-33.6	-9.7	13.62
TWC-3	dolomite	126	-33.7	-11.0	14.97
TWC-3	dolomite	120	-30.3	-9.8	13.72
TWC-3	dolomite	146	-46.5	-16.3	19.68
TWC-3	dolomite	125	-49.2	-16.7	19.99
TWC-3	dolomite	125	-39.6	-17.0	20.22
TWC-3	dolomite	142	-48.7	-15.2	18.80
TWC-3	dolomite	128	-44.4	-11.4	15.37
TWC-3	dolomite	121	-41.2	-10.8	14.77
TWC-3	dolomite	119	-35.0	-16.3	19.68
TWC-7	calcite	84	-33.8	-8.3	12.05
TWC-7	calcite	127	-23.5	-5.2	8.14
TWC-7	calcite	143	-25.4	-6.0	9.21
TWC-7	calcite	122	-30.1	-5.3	8.28
TWC-7	calcite	116	-31.9	-7.2	10.73
TWC-7	calcite	198	-28.4	-7.5	11.10
TWC-7	dolomite	164	-42.3	-10.1	14.04
TWC-7	dolomite	160	-38.3	-7.7	11.34
TWC-7	dolomite	148	-31.6	-6.8	10.24
TWC-7	dolomite	148	-38.7	-5.2	8.14
TWC-7	dolomite	212	-40.8	-10.6	14.57
TWC-7	dolomite	140	-35.6	-7.2	10.73
TWC-7	dolomite	146	-27.4	-7.5	11.10
TWC-7	dolomite	168	-39.5	-5.3	8.28
TWC-7	dolomite	152	-40.0	-8.0	11.70
TWC-7	dolomite	145	-40.2	-7.3	10.86
TWC-7	dolomite	149	-32.8	-5.8	8.95
TWC-7	dolomite	147	-27.2	-4.4	7.02
TWC-7	dolomite	136	-32.0	-7.8	11.46
TWC-7	dolomite	147	-43.8	-7.8	11.46
TWC-7	dolomite	140	-34.8	-4.5	7.17
TWC-7	dolomite	148	-33.2	-4.0	6.45
TWC-7	dolomite	150	-36.1	-6.9	10.36
TWC-7	dolomite	146	-29.1	-4.6	7.31
TWC-7	dolomite	140	-24.7	-4.9	7.73
TWC-7	dolomite	145	-29.3	-3.3	5.41
TWC-7	dolomite	144	-33.7	-5.1	8.00

Sample	Mineral	T_h	T_{fm}	T_m	wt.% equiv. NaCl (Tm)
TWC-7	dolomite	144	-31.6	-3.8	6.16
TWC-7	dolomite	131	-33.4	-4.3	6.88
TWC-7	dolomite	141	-25.7	-4.1	6.59
OD-1	quartz	149	-40.8	-7.7	11.34
OD-1	quartz	141	-37.8	-5.4	8.41
OD-1	quartz	134	-29.5	-9.6	13.51
OD-1	quartz	111	-39.5	-9.3	13.18
OD-1	quartz	113	-38.4	-9.4	13.29
OD-1	quartz	120	-32.5	-9.3	13.18
OD-1	quartz	129	-34.0	-6.6	9.98
OD-1	quartz	179	-36.6	-9.0	12.85
OD-1	quartz	187	-45.3	-6.3	9.60
OD-1	quartz	190	-39.5	-8.0	11.70
OD-1	quartz	195	-42.4	-8.1	11.81
OD-1	quartz	131	-39.5	-11.5	15.47
OD-1	quartz	224	-38.4	-12.3	16.24
OD-1	quartz	226	-51.7	-8.3	12.05
OD-1	quartz	240	-44.9	-12.8	16.71
OD-1	quartz	237	-34.9	-10.8	14.77
OD-1	quartz	185	-41.9	-9.3	13.18
OD-1	quartz	181	-38.5	-6.5	9.86
OD-1	quartz	120	-31.8	-9.7	13.62
OD-1	quartz	127	-42.4	-9.4	13.29
OD-1	quartz	133	-35.5	-9.1	12.96
OD-1	quartz	125	-38.5	-9.5	13.40
OD-1	quartz	181	-45.3	-9.8	13.72
OD-1	quartz	126	-35.2	-9.2	13.07
OD-1	quartz	202	-38.1	-8.7	12.51
OD-1	quartz	132	-35.5	-7.1	10.61
OD-3	dolomite	202	-47.9	-5.6	8.68
OD-3	dolomite	126	-45.7	-11.0	14.97
OD-3	dolomite	119	-50.6	-8.7	12.51
OD-3	dolomite	116	-50.3	-10.9	14.87
OD-3	dolomite	114	-45.9	-7.8	11.46
OD-3	dolomite	167	-42.1	-10.5	14.46
OD-3	dolomite	175	-34.4	-11.3	15.27
OD-3	dolomite	121	-43.8	-9.6	13.51
OD-4	calcite	115	-40.8	-5.4	8.41
OD-4	calcite	124	-35.2	-4.4	7.02
OD-4	calcite	107	N/A	-5.2	8.14
OD-4	calcite	108	N/A	-4.2	6.74

Sample	Mineral	T_h	T_{fm}	T_m	wt.% equiv. NaCl (Tm)
OD-4	calcite	111	-36.0	-6.1	9.34
OD-4	calcite	114	-43.3	-5.0	7.86
OD-4	calcite	126	-41.0	-5.0	7.86
OD-4	calcite	147	-30.8	-6.2	9.47
OD-4	calcite	112	-34.1	-7.8	11.46
OD-4	calcite	130	-48.6	-8.0	11.70
OD-4	calcite	135	-40.2	-5.5	8.55
OD-4	calcite	116	-40.7	-5.1	8.00
OD-4	calcite	155	-45.4	-7.3	10.86
OD-4	calcite	129	-37.2	-4.3	6.88
TAQ-1	fluorite	139	-27.6	-6.0	9.21
TAQ-1	fluorite	138	-28.1	-6.0	9.21
TAQ-1	fluorite	113	-27.4	-6.0	9.21
TAQ-1	fluorite	143	-29.4	-2.5	4.18
TAQ-1	fluorite	141	-30.0	-6.3	9.60
TAQ-1	fluorite	114	-29.2	-6.3	9.60
TAQ-1	fluorite	120	-24.6	-5.5	8.55
TAQ-1	fluorite	122	-24.3	-4.1	6.59
TAQ-1	fluorite	125	-25.2	-5.3	8.28
TAQ-1	fluorite	118	-25.9	-5.0	7.86
TAQ-1	fluorite	139	-21.2	-6.6	9.98
TAQ-1	fluorite	132	-19.6	-7.0	10.49
TAQ-1	fluorite	146	-21.0	-6.4	9.73
TAQ-1	fluorite	142	-20.0	-9.8	13.72
TAQ-1	fluorite	110	-21.4	-7.7	11.34
TAQ-1	fluorite	110	-24.9	-8.3	12.05
TAQ-1	fluorite	109	-26.8	-8.0	11.70
TAQ-1	fluorite	114	-26.1	-5.7	8.81
TAQ-1	fluorite	114	-23.3	-8.2	11.93
TAQ-1	fluorite	109	-23.9	-5.5	8.55
TAQ-1	fluorite	107	-23.3	-6.8	10.24
TAQ-1	fluorite	111	-25.7	-5.6	8.68
TAQ-1	fluorite	150	-26.7	-5.5	8.55
TAQ-1	fluorite	148	-23.7	-6.9	10.36
TAQ-1	fluorite	150	-24.0	-5.1	8.00
TAQ-1	fluorite	157	-23.4	-7.4	10.98
TAQ-1	fluorite	158	-26.8	-7.3	10.86
TAQ-1	fluorite	158	-20.8	-8.0	11.70
TAQ-1	fluorite	157	-22.0	-8.3	12.05
TAQ-1	fluorite	151	-23.0	-6.3	9.60
TAQ-1	fluorite	161	-28.6	-7.9	11.58

Sample	Mineral	T_h	T_{fm}	T_m	wt.% equiv. NaCl (Tm)
TAQ-1	fluorite	151	-26.6	-7.7	11.34
TAQ-1	fluorite	155	-22.9	-8.3	12.05
TAQ-1	calcite	150	-22.8	-4.3	6.88
TAQ-1	calcite	163	-35.0	-5.8	8.95
TAQ-1	calcite	192	-36.0	-3.9	6.30
TAQ-1	calcite	130	-21.5	-5.4	8.41
TAQ-1	calcite	142	-27.0	-8.3	12.05
TAQ-1	calcite	125	-25.8	-5.5	8.55
TAQ-1	calcite	150	-24.4	-4.9	7.73
TAQ-1	calcite	84	-27.7	-8.4	12.16
TAQ-1	calcite	88	-25.3	-7.8	11.46
TAQ-1	calcite	90	-26.0	-7.0	10.49
TAQ-1	calcite	119	-22.0	-8.8	12.62
TAQ-1	calcite	147	-23.0	-3.0	4.96
TAQ-1	calcite	131	-26.3	-6.3	9.60
TAQ-1	calcite	156	-23.8	-6.0	9.21
TAQ-1	calcite	123	-24.3	-5.4	8.41
TAQ-1	calcite	160	-25.4	-7.1	10.61
TAQ-1	calcite	223	-29.3	-15.7	19.21
TAQ-1	calcite	136	-24.0	-7.9	11.58
TA-1	calcite	147	-32.2	-5.2	8.14
TA-1	calcite	111	-26.8	-4.3	6.88
TA-1	calcite	127	-26.3	-5.6	8.68
TA-1	calcite	96	-22.0	-4.3	6.88
TA-1	calcite	84	N/A	N/A	N/A
TA-1	calcite	100	N/A	N/A	N/A
TA-1	calcite	101	-24.6	-6.6	9.98
TA-1	calcite	116	-24.2	-8.1	11.81
TA-1	calcite	112	-28.6	-5.7	8.81
TA-1	calcite	148	-21.8	-3.2	5.26
TA-1	calcite	127	-28.0	-4.5	7.17
TA-1	calcite	130	-24.6	-4.6	7.31
TA-1	calcite	90	-25.6	-8.1	11.81
TA-1	calcite	158	-22.5	-9.7	13.62

Appendix 4 – Carbon and oxygen isotope data

Stable isotope data from northwest Ireland. Values are expressed in per mil relative to VPDB.

Abbeytown

Sample Number	Sample Type	$\delta^{13}C$	$\delta^{18}O$	Sample Details
AT-1	host dolomite	3.64	-8.87	
AT-5	host dolomite	3.21	-9.60	
AT-7	host dolomite	2.95	-9.01	
AT-8	host dolomite	4.07	-9.19	
AM-4	host dolomite	3.33	-8.21	
AM-7	host dolomite	2.07	-9.86	
AM-8	host dolomite	3.33	-9.10	
AM-10	host dolomite	3.45	-9.36	
AM-11	host dolomite	3.31	-9.00	
AM-12	host dolomite	2.52	-8.19	
AT-3	host limestone	4.33	-6.56	
AT-12	host limestone	3.37	-6.67	
AM-3	host limestone	1.28	-8.98	
AT-4	dolomite cement	3.60	-5.39	main ore body
AT-5	dolomite cement	3.36	-7.34	main ore body
AT-9	dolomite cement	3.47	-7.40	main ore body
AM-9	dolomite cement	2.99	-9.49	western ore body
AM-11	dolomite cement	2.11	-10.92	western ore body
AM-12	dolomite cement	2.94	-8.57	western ore body
AT-2	calcite cement	1.06	-10.31	main ore body
AT-4	calcite cement	2.34	-7.88	main ore body
AT-5	calcite cement	0.83	-10.67	main ore body
AT-9	calcite cement	1.03	-10.05	main ore body
AM-8	calcite cement	1.41	-10.29	main ore body
AT-12	calcite cement	1.58	-9.10	western ore body
AM-9	calcite cement	0.57	-13.52	western ore body
AM-12	calcite cement	0.52	-10.69	western ore body
AM-13	calcite cement	0.91	-10.49	western ore body

TQ/TWC

Sample Number	Sample Type	$\delta^{13}C$	$\delta^{18}O$	Sample Details
TW-1	host dolomite	2.37	-8.97	
TWC-3	host dolomite	3.32	-7.86	
TWC-7	host dolomite	3.62	-8.59	
TQ-5	host limestone	3.40	-6.70	

Sample Number	Sample Type	$\delta^{13}C$	$\delta^{18}O$	Sample Details
TQ-7	host limestone	3.96	-4.66	
TQ-2	dolomite cement	3.38	-4.39	extra CL zones
TW-3	dolomite cement	0.70	-10.50	extra CL zones
TWC-1	dolomite cement	1.59	-12.66	2 zone CL
TWC-10	dolomite cement	1.08	-12.83	2 zone CL
TWC-3	dolomite cement	1.06	-12.89	extra CL zones
TWC-5	dolomite cement	1.42	-12.21	2 zone CL
TWC-7	dolomite cement	1.59	-9.45	extra CL zones
TWC-8	dolomite cement	0.10	-10.60	2 zone CL
TQ-7	calcite cement	3.18	-7.12	marine cement
TQ-7	calcite cement	3.11	-9.03	vein
TR-1	calcite cement	2.95	-9.22	
TW-1	calcite cement	0.32	-11.53	
TWC-3	calcite cement	0.43	-11.08	
TWC-11	calcite cement	1.37	-13.32	

O'Donnell's Rock

Sample Number	Sample Type	$\delta^{13}C$	$\delta^{18}O$
OR-2	host dolomite	2.57	-7.06
OD-3	host dolomite	3.23	-5.41
OD-4	host limestone	2.47	-5.74
OR-2	dolomite cement	2.20	-9.20
OD-3	dolomite cement	2.88	-8.45
OR-2	calcite cement	1.35	-10.37
OD-4	calcite cement	2.33	-6.55

Tate's Quarry

Sample Number	Sample Type	$\delta^{13}C$	$\delta^{18}O$
TAQ-1	host limestone	3.68	-5.35
TA-1	host limestone	3.32	-5.07
TA-3	host limestone	3.27	-4.26
TAQ-1	calcite cement	3.07	-5.66
TA-1	calcite cement	3.03	-9.15

VITA

Christopher J. Persellin

Candidate for the Degree of

Master of Science

Thesis: DOLOMITIZATION AND SULFIDE MINERALIZATION OF LOWER CARBONIFEROUS STRATA, NW IRELAND

Major Field: Geology

Biographical:

Personal Data: Born in Houston, Texas, on November 19, 1983, the son of James and Patricia Persellin.

Education: Graduated from Flowing Wells High School, Tucson, Arizona in May 2002; received Bachelor of Science degree in Geological Sciences from Arizona State University, Tempe, Arizona in May 2006. Completed the requirements for the Master of Science degree in Geology at Oklahoma State University, Stillwater, Oklahoma in May 2009.

Experience: Employed by Oklahoma State University, Boone Pickens School of Geology as a graduate teaching assistant from 2006 to 2008; employed by EOG Resources as a Geology Intern, summer 2008.

Professional Memberships: Geological Society of America, American Association of Petroleum Geologists

Name: Christopher J. Persellin Date of Degree: May, 2009

Institution: Oklahoma State University Location: Stillwater, Oklahoma

Title of Study: DOLOMITIZATION AND SULFIDE MINERALIZATION OF LOWER CARBONIFEROUS STRATA, NW IRELAND

Pages in Study: 91 Candidate for the Degree of Master of Science

Major Field: Geology

Scope and Method of Study: The Pb-Zn sulfide mineralization at Abbeytown Mine and Twigspark Quarry comprise the only known carbonate-hosted base-metal sulfide deposits in the Sligo Syncline, northwest Ireland. Prior studies at Abbeytown Mine have suggested that mineralizing fluids were derived regionally and were present throughout the Sligo Syncline. This study examined mineralization at Abbeytown, Twigspark and two additional locations in northwest Ireland to determine the origins and regional extent of mineralizing fluids. An emphasis was placed on establishing geographic and stratigraphic relationships to determine if and to what extent regional fluid migration was present during diagenesis.

Findings and Conclusions: Host limestone sedimentation occurred concurrently throughout the region as indicated by field relationships and petrography; however petrographic and stable isotope evidence indicates host rock dolomitization occurred under differing conditions at localities to the west of the Ox Mountains Inlier and localities to the east of the Inlier, suggesting significant uplift and geologic isolation of these areas prior to dolomitization. Localized fluid flow systems are responsible for sulfide mineralization and associated epigenetic carbonate cements. West of the Ox Mountains Inlier at Abbeytown three geochemically distinct fluids are observed: 1) a lower-temperature, lower-salinity fluid (70-130 °C, 4-9 wt. % equiv. NaCl); 2) a lower-temperature, higher-salinity fluid (70-140 °C, 15-24 wt. % equiv. NaCl); and 3) a higher-temperature, moderate-salinity fluid (165-220 °C, 8-14 wt. % equiv. NaCl). Three similar fluid types were observed at nearby Twigspark Quarry. The source of the high-salinity fluid is likely seawater evaporated to near the point of halite precipitation. The higher-temperature fluid is thought to be derived from deep circulation of basinal brines. It is speculated that the interaction of the higher-salinity fluid with the higher-temperature fluid was vital for ore formation. Less complex fluid flow systems are indicated for sites east of the Ox Mountains Inlier where no sulfide mineralization was observed.

ADVISER'S APPROVAL: Dr. Jay M. Gregg